International Journal of Concrete Structures and Materials

RESEARCH Open Access

Using Optimization Techniques on Mechanical Characteristics and Sustainability Assessment of Rubberized Concrete Blended with PVA Fiber Through Response Surface Methodology

Naraindas Bheel[1], Abhijeet Vidyadhar Baikerikar[1] and Bashar S. Mohammed[1*]

Abstract

The construction sector is promoting eco-friendly materials to combat global warming. Researchers use crumb rubber (CR) in concrete due to its ductility and hardness, but studies show it can decrease strength. Therefore, the addition of PVA fiber improves the mechanical properties of CR concrete. The research aims to assess the mechanical and physical characteristics of concrete by utilizing RSM modeling and optimization, comparing the effects of CR replacement for sand and PVA fiber by volume fraction. It has been observed that the optimum compressive, tensile and flexural strengths were observed by 49 MPa, 4.31 MPa, and 5.88 MPa at 10% of sand replaced with CR and 1.5% of PVA fiber together at 28 days, respectively. In addition, water absorption improves with increased CR and PVA fiber in concrete, while dry density decreases with increased CR and PVA fiber quantity in concrete at 28 days, respectively. Moreover, RSM was utilized to develop response prediction models with R^2 coefficients ranged from 97 to 99%. Furthermore, the enhancement of embodied carbon is seen when the volume percent of PVA fiber and CR increases in concrete. Additionally, using 10% CR instead of sand and adding 1.5% PVA fiber has been proven to deliver favourable outcomes for the construction sector therefore it is recommended for construction purpose.

Keywords Concrete, Crumb rubber, PVA fiber, Mechanical properties, Embodied carbon, RSM modeling and optimization

1 Introduction

In recent times, because of the fast growth of the transportation sector, the problem of waste tires has emerged as a critical concern for several nations. Tires reached a point in their lifecycle where they may no longer be utilized and are ultimately disposed of as garbage (Eisa et al., 2020). However, millions of tires that are no longer usable and they are disposed of annually (Abdullah et al., 2024).

The environmental effect of discarded tires may vary depending on the area's waste management program. Some circumstances may turn them into a significant environmental hazard, while others may turn them into a valuable source (Magagula et al., 2023). The dumping of waste tires on land leads to significant economic and environmental issues, as revealed in prior study (Najim & Hall, 2010). In addition to posing a possible environmental risk, the dumping issues also have the potential to trigger accidental fires that emit pollution, which can be difficult to manage owing to the tires' high flammability.

*Correspondence:
Bashar S. Mohammed
bashar.mohammed@utp.edu.my
[1] Department of Civil and Environmental Engineering, Universiti Teknologi PETRONAS, 32610 Bandar Seri Iskandar, Perak, Malaysia

Moreover, they offer conducive environments for the proliferation of mice, mosquitoes and rats (Abdullah et al., 2024). In recent decades, the appropriate disposal of tires has arisen as a significant environmental issue. Subsequently, investigators have conducted several investigations to evaluate various tire disposal techniques (Batayneh et al., 2008; Mahlangu, 2009). As a result, landfilling has turned into an unacceptable option owing to the growing exhaustion of viable places for garbage disposal. Consequently, several governments have implemented stringent legal measures to prevent the production of tires in landfills. Efforts to address the problem of tire disposal have included the continuous development of innovative methods. A number of measures show promise: the reuse of tire rubber material in asphaltic mixtures for concrete (Shu & Huang, 2014), the accumulation of tire rubber into concrete (Toutanji, 1996), the combustion of tires for producing steam, and the recycling of ground tire rubber in several rubber and plastic objects (Eisa et al., 2020).

Scientists have conducted extensive study on the integration of crumb rubber, derived from used tires, into concrete (Aghamohammadi et al., 2024; Qaidi et al., 2021; Ren et al., 2022; Siddika et al., 2019; Singaravel et al., 2024). CR is the result of reducing and grinding scrap tires into tiny particles, frequently varying from 4.75 mm to 75 μm (Eisa et al., 2020). Investigations have revealed that using CR with average sizes of particles fluctuating from 1 to 4 mm has shown satisfactory qualities for concrete (Bing & Ning, 2014; Gesoğlu et al., 2014; Onuaguluchi & Panesar, 2014). In the past era, the incorporation of crumb rubber (CR) in concrete as a substitute for aggregate has been widespread due to its notable characteristics such as relatively low density and excellent ductility (Ismail & Hassan, 2016; Khaloo et al., 2008; Sgobba et al., 2015; Zheng et al., 2008). Roughly 1000 million tires reach the end of their operational lifespan per annum due to the growth of the vehicle industry. Over 50 percent of these tires are disposed of without any treatment, posing a significant hazard to our natural environment (Thomas et al., 2016; Xiong et al., 2021). Rubberized concrete, a significant approach for recycling utilized tires, has been extensively researched by several authors (Batayneh et al., 2008; Li et al., 2016; Liu et al., 2013; Long et al., 2018; Shu & Huang, 2014; Son et al., 2011; Zhong et al., 2019). CR produced by destroying garbage tires and it can be applied as substitution for sand in traditional concrete. This practice helps recycle tires, lessen the requirement of natural aggregates, and promote sustainability while sustaining the ecosystem (Long et al., 2018; Thomas et al., 2016). Rubberized concrete has enhanced engineering characteristics in comparison to traditional concrete, including increased toughness, greater impact resistance, enhanced absorption of energy resources, and more effective abrasion resistance (Batayneh et al., 2008; Li et al., 2016; Liu et al., 2013; Long et al., 2018; Shu & Huang, 2014; Son et al., 2011; Zhong et al., 2019). CR concrete has many potential applications in construction sector due to its outstanding characteristics. Rubberized concrete is a durable substance with superior flexibility and resistance to impact, making it suitable for many applications such as impact hurdles, building materials, pavements, playing area surfaces, and anti-collision foundations (Batayneh et al., 2008; Shu & Huang, 2014; Son et al., 2011). Rubberized concrete's effective dissipating energy capability allows for its use in enhancing the earthquake resistance of concrete buildings (Dehdezi et al., 2015). However, the flexural strength (FS), tensile strength (TS), and compressive strength (CS) of rubber-based concrete are inferior to those of traditional concrete (Li et al., 2016; Zhong et al., 2019). Incorporating fibers into concrete is a beneficial method for enhancing the FS, TS and CS of the material. Several studies have examined how various types of fibers, like polypropylene (PP), steel fiber, nylon fiber, polyvinyl alcohol (PVA) fiber, basalt fiber, and jute fiber, impact the mechanical characteristics of CR concrete construction. Fibers augment the FS and durability of concrete by providing bridging behavior, which has been demonstrated in several studies (Al-Hadithi et al., 2019; Hesami et al., 2016; Wang et al., 2018; Zhong et al., 2019).

The characteristics of rubberized concrete have been extensively researched with the introduction of PVA fiber (Li et al., 2001, 2002; Wang et al., 2018). The study found that PVA fiber is very suitable for reinforcing rubberized concrete. The study identified PVA fiber as a very appropriate polymeric fiber for strengthening rubberized concrete. Fiber-reinforced concrete (FRC) is often applied in various purposes, such as precast construction elements, concrete floor coverings, and outstanding-durability concrete (Alhozaimy et al., 1996; Anas et al., 2022; Li et al., 2001). Internal fractures' propagation influences either the tensile strength or bending resistivity of concrete construction. Whenever fractures are restricted locally by a surrounding matrix, the onset of fractures may be delayed, and stronger concrete can be produced (Alhozaimy et al., 1996). Incorporating robust fibers into concrete helps reduce the development of cracks. Besides, PVA fibers possess an outstanding modulus of elasticity and strong tensile strength. Scientists have demonstrated that PVA–cementitious composites not only have higher tensile strength but also offer improved fatigue resistance, stiffness, and longevity of cementitious composites. These composites also demonstrate a strain hardening tendency, with failure stresses reaching up to 4% in some instances (Li et al., 2002; Naggar & Abdo, 2023).

Moreover, many investigations were conducted on CR concrete and PVA fiber individually for determining the mechanical and durability properties. But there is limited experimental work performed on CR concrete combined with numerous concentrations of PVA fiber to determine the mechanical characteristics and embodied carbon of CR concrete. Therefore, the purpose of this research is conducted on the mechanical characteristics and sustainability assessment of CR concrete mixed with numerous amounts of PVA fiber by applying RSM modeling and to optimize the input and output parameters for practical application of the construction industry.

2 Experimental program

2.1 Materials

Portland Cement (PC) Type I was used in research by using ASTM C 150 (ASTM C150 & C150M-16e1, 2016) standards and the XRF of PC is shown in Table 1. However, the river sand with specific gravity of 2.64 which passes through 4.75-mm sieve while the coarse aggregates (CA) with a 2.66 specific gravity having 20 mm in size used in research work. In addition, the crumb rubber (CR) with a 0.92 specific gravity passes from 1.18 mm sieve and it used as a partial replacement for sand by volume. Moreover, polyvinyl alcohol fiber (PVA) was included in the concrete based on its volume percent of concrete and surface of fiber was treated with 1.2% oil by the weight of the fiber to control the fiber/matrix interfacial properties (Abdulkadir et al., 2021a, 2022; Bheel et al., 2023a; Mohammed et al., 2020). Table 2 provides the characteristics of PVA fiber. Furthermore, the superplasticizer (SP) was added to the rubberized concrete to improve the flow of the fresh mix. In addition, drinking water was utilized to make the concrete and cure the rubberized specimens.

2.2 Response surface methodology (RSM) modeling

It is a statistical and mathematical approach applied to model and analyze issues where numerous input factors have an impact on the outcome variable. RSM modeling is an efficient step-by-step approach to optimizing procedures and understanding the connections between many input features and a response parameter. The first step entails precisely describing the issue, including the aim, input parameters (factors), and response parameters (outputs). Afterward, a suitable experimental design, like Central Composite Design (CCD) or Box–Behnken design (BBD), is selected, and the specific values for each factor are established. Then, experiments are carried out based on this design, methodically altering the input parameters and documenting the related outcomes. The gathered data are used to generate a polynomial regression approach, often a second-order approach, that accurately portrays the connection between the inputs and the output. Model validation involves using statistical assessments like ANOVA, residual analysis, and lack-of-fit assessments to determine the model's suitability. After being verified, response surface diagrams, including contour and 3D diagrams, are created to visually represent the relationships between parameters. Optimization approaches, like gradient descent or the approach of steepest ascent, are utilized to analyze the response surface and determine the most favourable values for the input parameters. Finally, confirmation runs are performed using these ideal parameters to validate the anticipated outcome, guaranteeing the correctness and dependability of the model. This comprehensive methodology enables efficient process optimization and a more profound comprehension of variable interrelationships.

2.3 RSM modeling generated mix proportions

The RSM modeling was used to produce 13 runs of various mixture by considering two input factors (CR and PVA fiber) for this research. The variables were fluctuated at three levels: CR (0%, 10%, 20%, and 30% substitution by volume of FA) and PVA fiber (1%, 1.5%, and 2% inclusion by volume percentage of concrete). The design had 13 different combinations with five repeated central

Table 1 Chemical constituents of PC

Materials	Compound (%)									Specific gravity	Blaine fineness (m^2/kg)	Loss on ignition
	SiO_2	Fe_2O_3	Al_2O_3	CaO	MnO	Na_2O	MgO	T_2O	K_2O			
PC	20.76	3.35	5.54	61.4	–	0.19	2.48	–	0.78	3.15	325	2.20

Table 2 PVA fiber properties (Abdulkadir et al., 2021b)

Category	Grade	Diameter	Length	Aspect ratio (l/d)	SG	Modulus of elasticity	TS
PVA	REC S-15	40 µm	12 mm	462	1.3	41 GPa	1600 MPa

elements and these five repeated central mixtures are written in MCP form in all data graphs. Many researchers have observed this approach (Al-Fakih et al., 2020; Jo et al., 2015; Khed et al., 2020). To study the mechanical (CS, TS, and FS) and physical (dry density and water absorption) properties of rubberized concrete, the RSM program made 13 different mixes by changing the variables. Table 3 displays the combinations and specific of each composition.

2.4 Mixing procedure

The mixing process was conducted according to the standardized concrete mixing technique, as described by BS 1881: Part 125:1986 standard procedure. With the exception of PVA fiber, the dry components of the CR, sand, coarse aggregates, and cement, were combined in a dry condition utilizing a pan-type concrete mixer for a duration of 2 min at a low load speed of 30 RPM. A solution of water and SP was added to the dry mixture and allowed to circulate for an additional 3 min at a high speed of 80 RPM. Ultimately, the PVA fiber was progressively included in the mixture with a rotational speed of around 30 to 60 RPM, ensuring even dispersion and preventing the formation of fiber clumps. The mixer was operated for a further 5 min until a visually uniform mixture without any fiber clumps was achieved. The recently prepared CR concrete was thereafter put into the suitable, lightly lubricated molds. Once the specimens had reached a satisfactory level of strength after 24 h, they were removed from the molds and put in a curing tank for a period of 28 days to complete the curing process.

2.5 Testing procedure

The study examined the mechanical characteristics and physical parameters of rubberized mixture combined with different amounts of PVA fiber. The 100 mm × 100 mm × 100 mm cube samples were tested for CS by using BS EN 12390–3 (BS EN, 12390-3 2009) code at 7, 14 and 28 days. Besides, the TS was achieved on CR concrete samples shaped like a dog bone, with dimensions of 420 mm × 120 mm × 30 mm, following the protocol described in JSCE (Japan Society of Civil Engineers, 2008). A four-point bending test was conducted on beam (500 × 100 × 100 mm) for determining the FS by applying BS EN 12390–5 (BS EN, 12390-5 2009). Moreover, dry density was measured on cubic specimens by following the BS EN 12390-7 (British Standards Institution & BS EN, 12390 7:2000 2000) specification and the cube samples were tested for water absorption in accordance with BS 1881–122 (BS 1881: Part 122: 1983 Part 122 n.d.). These all testing was tested at 28 days. Figure 1a–d displays the experimental arrangement utilized in research.

3 Results and discussion

3.1 Compressive strength (CS)

For every mixture, a CS assessment was performed on PVA-CR concrete samples and these samples were tested on 7, 14, and 28 days. The outcomes of adding 10%, 20%, 30%, and 1%, 1.5 percent, and 2% of CR and PVA fibers, correspondingly, are displayed in Fig. 2. It is found that mixture with 10% of crumb rubber and 1.5% of PVA fibers gives the highest CS 26.46 MPa, 42.63 MPa, and 49 MPa at the end of 7, 14 and 28 days correspondingly. Similarly, it can be noted mixture with 30% CR and 2%

Table 3 Mix proportions of rubberized concrete developed by RSM modeling

Mix ID	Constituents (%)			Quantity of ingredients utilized in CR mixture (kg/m^3)				
	PVA	CR	PC	CA	Sand	CR	SP	Water
M0	0	0.00	475	1180	550	0	4.75	132
M1	1	10	475	1180	513.80	36.20	4.75	132
M2	1.5	10	475	1180	513.80	36.20	4.75	132
M3	2	30	475	1180	441.41	108.59	4.75	132
M4	1.5	20	475	1180	477.61	72.39	4.75	132
M5	1.5	20	475	1180	477.61	72.39	4.75	132
M6	1.5	20	475	1180	477.61	72.39	4.75	132
M7	2	20	475	1180	477.61	72.39	4.75	132
M8	1	20	475	1180	477.61	72.39	4.75	132
M9	1.5	30	475	1180	441.41	108.59	4.75	132
M10	1.5	20	475	1180	477.61	72.39	4.75	132
M11	1	30	475	1180	441.41	108.59	4.75	132
M12	2	10	475	1180	513.80	36.20	4.75	132
M13	1.5	20	475	1180	477.61	72.39	4.75	132

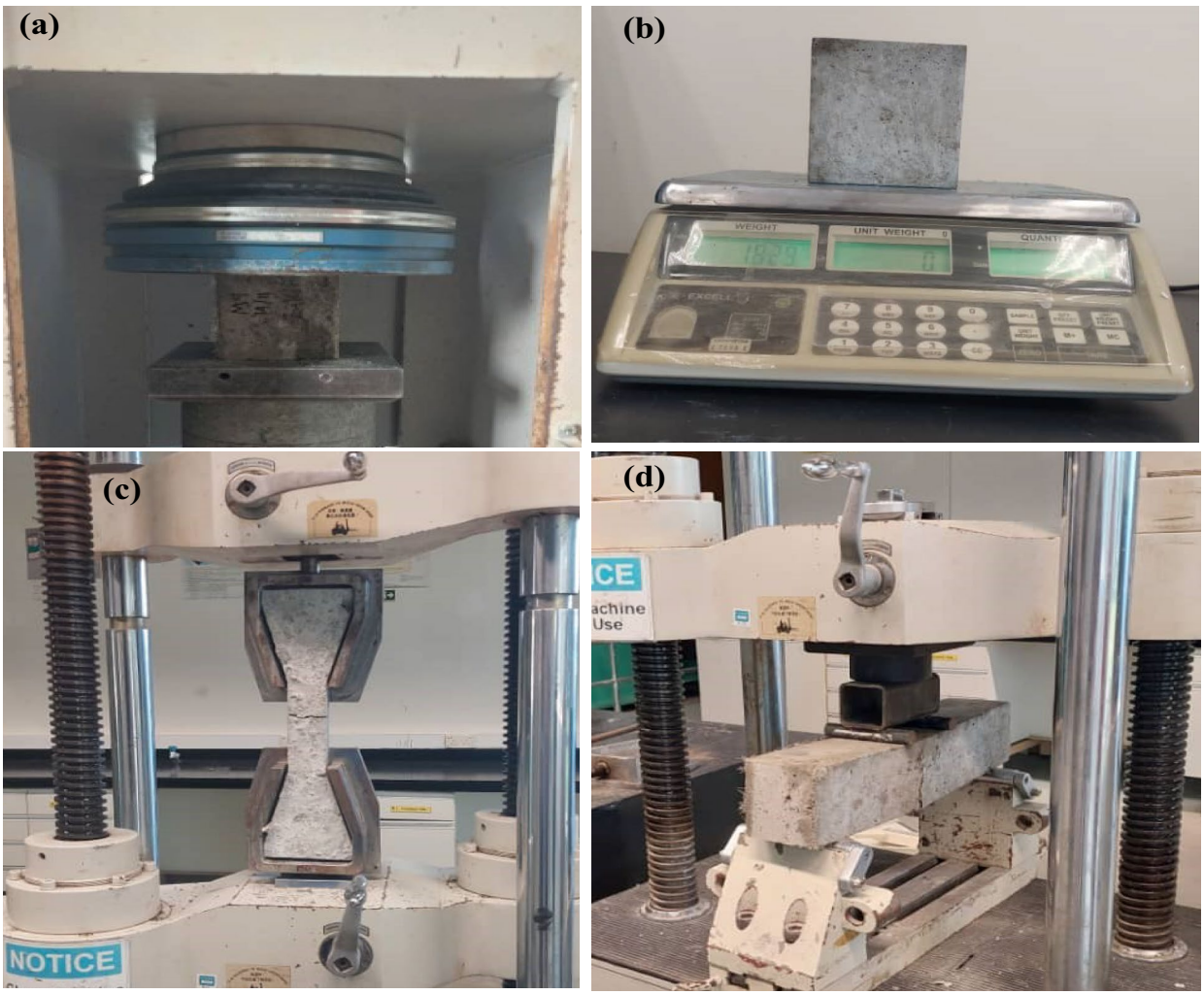

Fig. 1 Experimental setup of this research for **a** CS, **b** dry density, **c** TS, and **d** FS

PVA fibers gives the least CS 18.09 MPa, 29.14 MPa and 33.5 MPa at 7 days, 14 days and 28 days, correspondingly. It is noted that CS declines with the increase in CR, (Bisht & Ramana, 2017) shows similar results with the use of CR. A 6.21% increase in strength can be observed while 10% of sand is substituted with CR alone with 1.5% PVA fibers. Furthermore, it can observe an overall reduction in compressive strength of 37.5% using 30% CR and 2% PVA fibers than CM. This decrease can be due to the smooth surface texture of CR (Dong et al., 2013; Gupta et al., 2014; Meyyappan et al., 2023; Mohammed & Adamu, 2018) observed reduction in CS owing to rise in CR as more voids are produced by the addition of CR. Researchers (Benazzouk et al., 2007) showed the lightweight of the rubber at higher substitution level becomes increasingly more difficult to avoid voids, and due to the larger volume of fibers in the mixture, vibration becomes more difficult and more voids are created, it is one of the reasons for the reduction in CS. A similar studies have shown the reduction in strength owing to increment in the volume of fibers (Bheel et al., 2023b; Noushini et al., 2013).

3.2 Tensile strength

The TS of the combinations with varying amounts of PVA fiber and crumb rubber is displayed in Fig. 3. It is observed that out of all the mixtures, M2 mixture with 10% CR and 1.5% PVA fibers shows increase of 6.52% in TS compared to normal mix. The minimum TS can be perceived in the M3 mixture of 30% CR and 2% PVA fibers, a total decrease of 37.31% compared to normal mix and 46.26% decrease compared to M2 mix. The outcomes are in line with most of the studies (Aslani et al., 2018; Hossain et al., 2019; Mohammed et al., 2020; Shahjalal

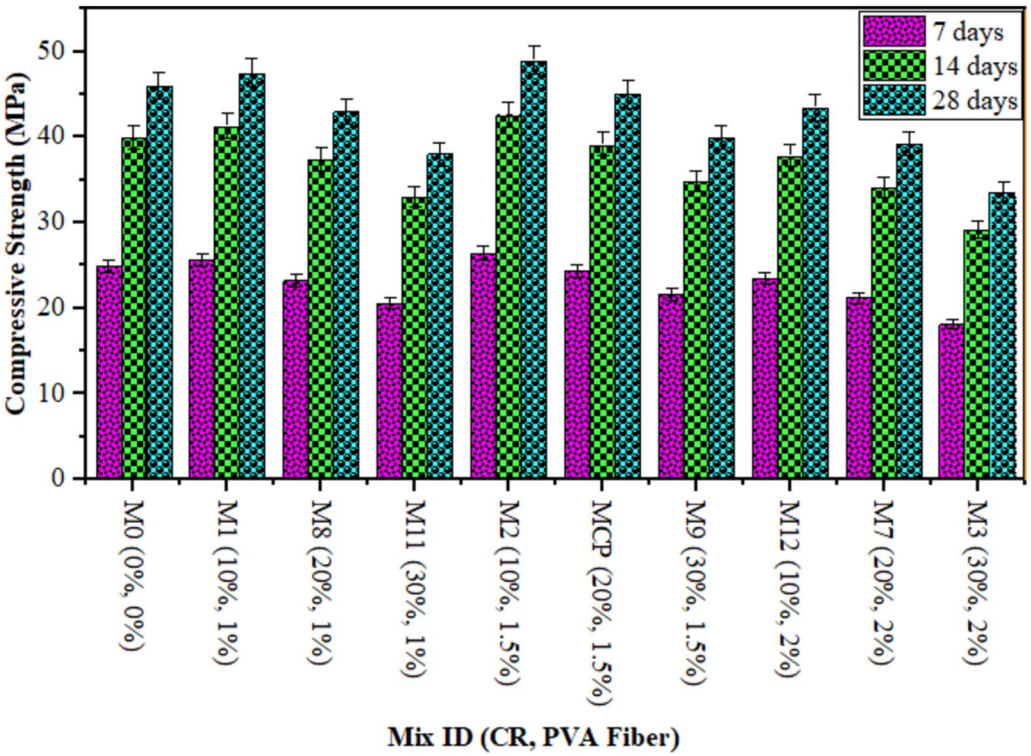

Fig. 2 Compressive strength of CR concrete combined with PVA fiber

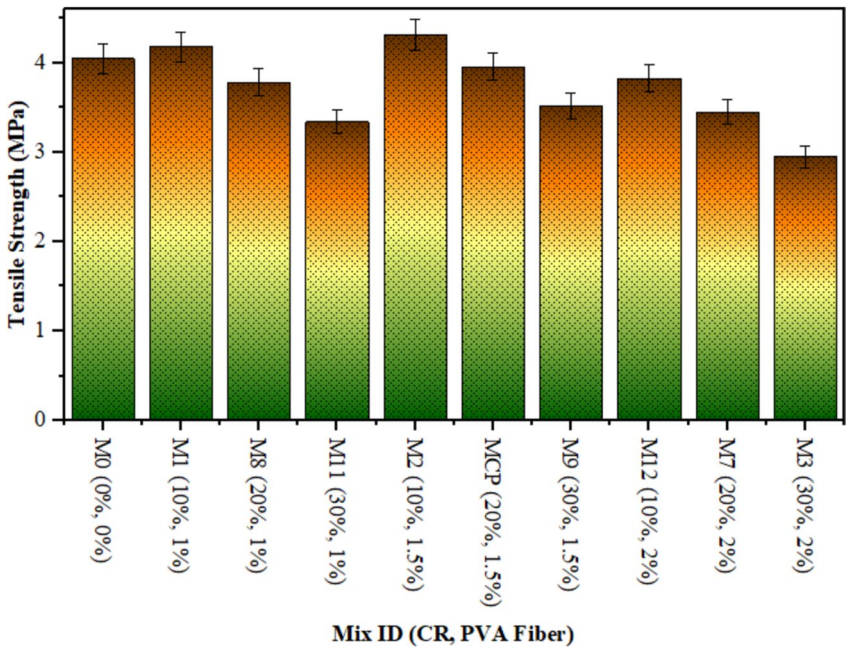

Fig. 3 TS of CR concrete blended with PVA fiber

et al., 2021) showed decrease in TS with the rise in fiber content but (Tamanna et al., 2020) shows the increment in the tensile strength up to 11% which is a similar trend as shown in Fig. 3. The fibers' ability to carry and distribute tensile stresses along cracks increases the concrete's tensile capacity, which is primarily responsible for the increase in TS. Due to stress reduction in the transition phase of the aggregates and rubber and overall strength is dropped when the content of CR increases (Hesami et al., 2016). Furthermore, Fig. 4 illustrates the relationship between CS and TS of CR concrete with varying volume fractions of PVA fiber after 28 days. The correlation between TS and CS at the 28-day mark is clearly depicted in Fig. 4. The equations presented in Fig. 4 could potentially be utilized to compute either CS or TS, given knowledge of one of these variables.

3.3 Flexural strength (FS)

A FS assessment was carried out for all mixtures. The outcomes are shown in Fig. 5. The FS of concrete increases gradually. For M1, a mixture of 10% rubber crumb and 1% PVA fibers, an increase of 3.2% can be observed compared to the nominal mixture. For M2, a mixture of 10% rubber crumbs and 1.5% PVA fibers, an increase of 6.52% is observed compared to the control combination. Subsequently, a reduction in FS is monitored for all other combinations. The increase in strength can be associated to the particle size of CR, as the smaller particles act as a filler in mixture, increasing the overall compactness of the concrete and reducing fractures which is also observed by Li et al. (2016) in their study. It is observed a decrease in FS with increased rubber content due to the smooth surface texture of the rubber, which cannot form a proper bond with the cement-based constituent in concrete, similar to the study conducted by Su (2015). The addition of PVA fibers plays an important role in developing FS. As content of fiber rises in CR concrete, the FS increases, which is consistent with studies conducted by Hesami et al. (2016); Hossain et al., 2019). The increase is due to the interlocking property of the fibers which is responsible for the bridge between mortar and aggregate but due to the increased content of CR flexural strength declines even with the rise in fibers (Chen et al., 2020; Xie et al., 2015). In addition, Figs. 6 and 7 depict the interplay between FS, CS, and TS in CR concrete, featuring different volume fractions of PVA fiber over a 28-day period. The graphical representation in Figs. 6 and 7 effectively showcases the relationship between FS, CS, and TS after 28 days. The formulas highlighted in Figs. 6 and 7 may serve as useful tools for calculating either FS, CS, or TS when one of these parameters is known.

3.4 Water absorption (WA)

Figure 8 demonstrations the diagram between the water absorption of different mixtures of rubber granules and PVA fiber concrete. The concrete sample without rubber crumbs and fibers was found to have low WA compared to all other mixes. The incorporation of more rubber crumbs and fibers increased the WA of CR concrete samples. The increased WA is due to the

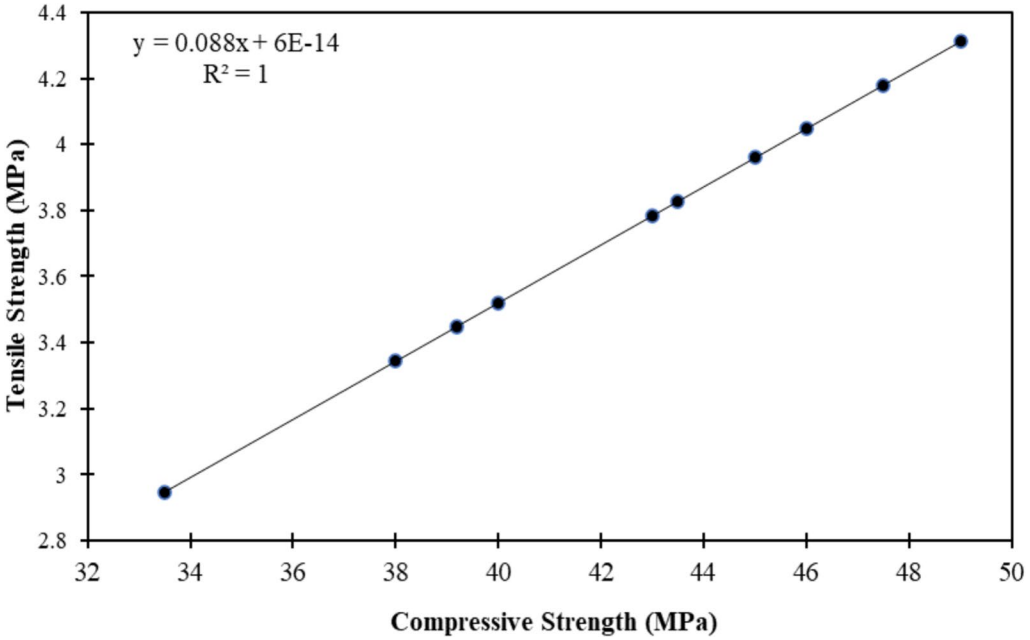

Fig. 4 Correlations between CS and TS of CR concrete containing PVA fiber

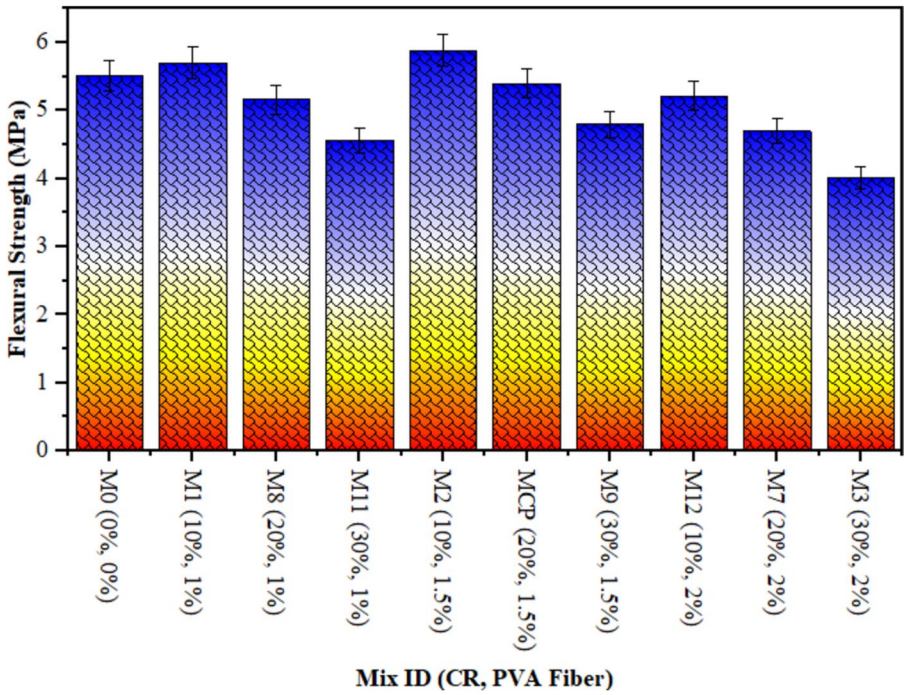

Fig. 5 Flexural strength of concrete

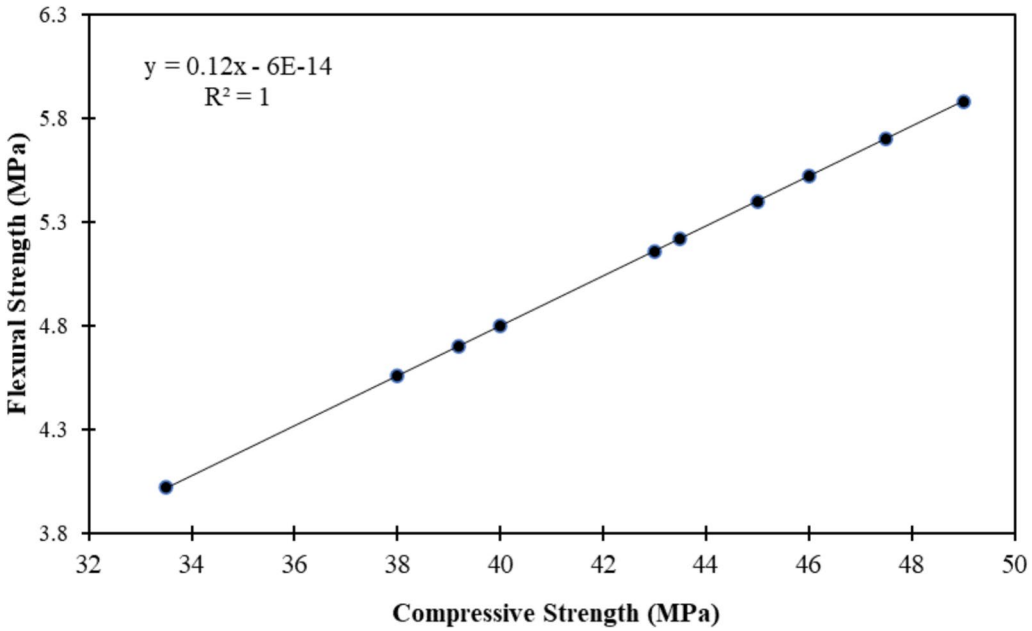

Fig. 6 Correlations between CS and FS of CR concrete containing PVA fiber

formation of pores and cracks in ITZ between rubber and cement mortar, which allows water to flow and this is supported by various studies (Bisht & Ramana, 2017; Gheni et al., 2017; Girskas & Nagrockienė, 2017; Youssf et al., 2017). However, studies (Alwi Assaggaf et al., 2022; Gonen, 2018; Pham et al., 2018) show that with minimal rubber crumb and controlled particle size, water absorption tends to be reduced due to proper void packing, making the concrete more compact and

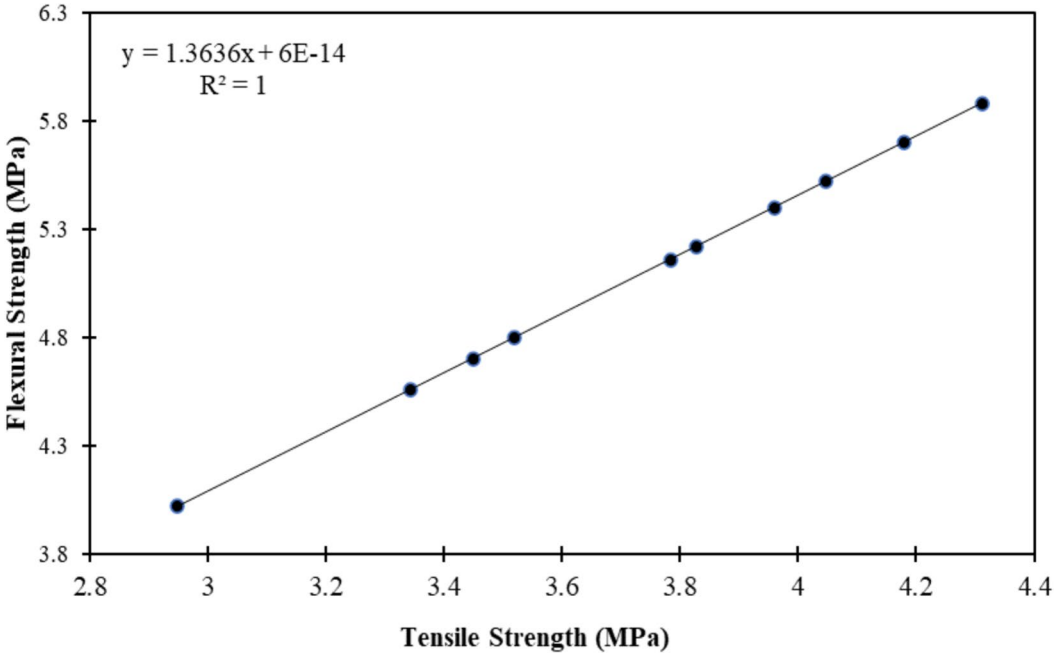

Fig. 7 Correlations between TS and FS of CR concrete containing PVA fiber

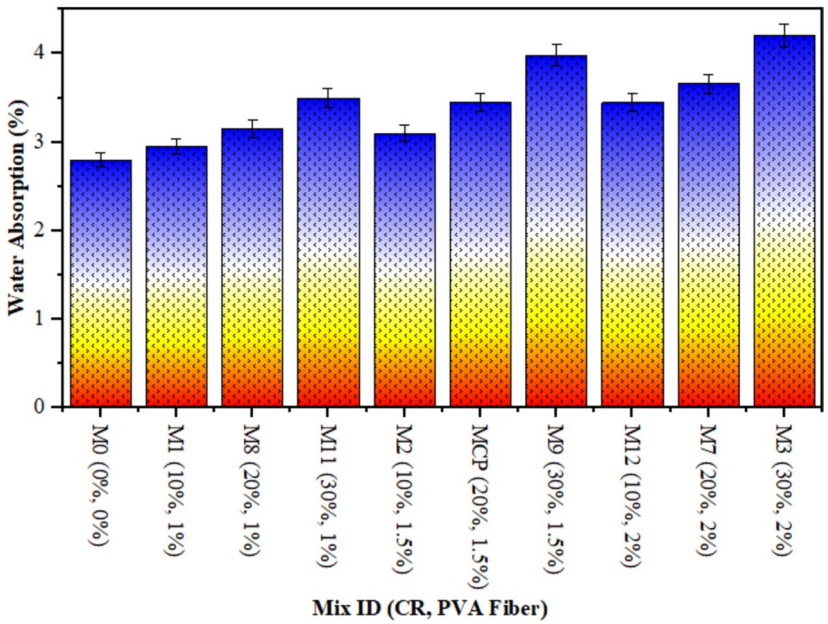

Fig. 8 Water absorption of CR concrete containing PVA fiber

making it more difficult for water to penetrate through the concrete. Fibers do not play a significant role in reducing WA as cracks and voids were present in the concrete, as a similar study argues with the above trend (Zia & Ali, 2017).

3.5 Dry density (DD)

Figure 9 shows the calculated dry density for all mixes containing crumb rubber and PVA fibers, as well as for concrete without crumb rubber and PVA fibers. It is clear from Fig. 9 that as the proportion of CR and fibers increases, the density decreases. It is observed a drop in

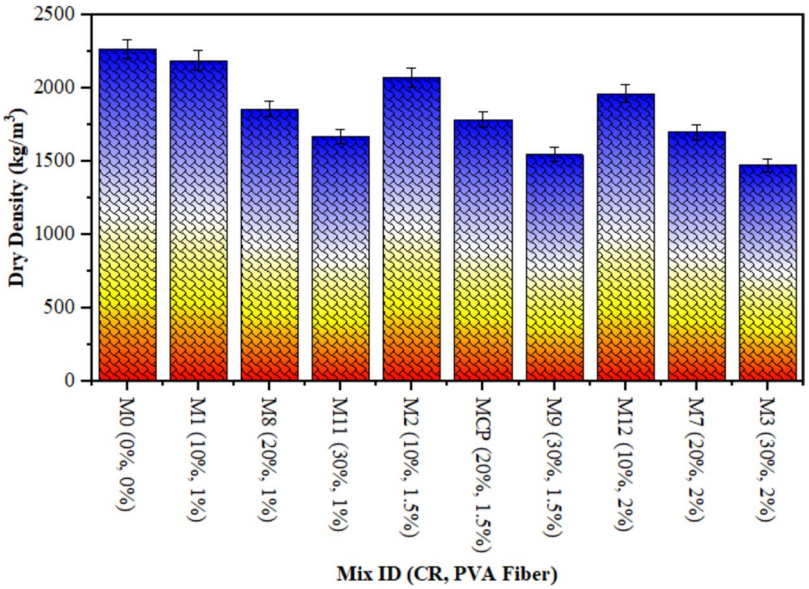

Fig. 9 Dry density of concrete

density by 35.8% in M11, 46.32% in M9 and 53.76% in M3. This is because the density of rubber and fibers is low associated to other ingredients of the concrete mix. The other reason justifying this result is that porosity and air spaces increased due to improper compaction, which created difficulties due to increased rubber and fiber content which also has adverse impact on CS of matrix (Zhang & Aslani, 2021). The researchers reported similar findings in their study as fiber content is increased density decreases along with studies carried out by Bheel et al., 2021a; Meddah & Bencheikh, 2009).

3.6 Field emission scanning electron microscopy (FESEM) analysis

The mechanical characteristics of CR concrete were improved with addition of PVA fiber in this research work. To get a deeper understanding of this enhancement procedure, rubberized concrete specimens with different concentrations of PVA fiber, especially 1%, 1.5%, and 2%, were selected for microscopic characteristic investigation. Figure 10 presents the results of the FESEM evaluation for specific samples of CR concrete that were reinforced with different amounts of polyvinyl alcohol (PVA) fiber. Figure 10a illustrates the quantity of pores in the control specimens. Researchers have recently identified a lot of micropores throughout the concrete mixture, leading to a decrease in its load-bearing capability. Figure 10b shows the bridging effect of 1% PVA fiber which is covered with C-S–H gel which reduced the inter-transitional zone (ITZ) of CR-concrete and make the stiff concrete that results in enhancing the strength of concrete. In addition, the specimens in the CR group had a substantial number of openings. As shown in Fig. 10c, 30% of CR involvement resulted in an increase in the number of microscopic fractures inside the concrete which results in reducing strength of concrete. Figure 10c shows that CR's hydrophobic properties caused a significant decrease in the concrete's interfacial transition zone (ITZ) strength. Previous research (Shao et al., 2021; Zhu et al., 2019) has shown comparable findings. The primary factor contributing to the reduced mechanical strength of CR concrete is its fundamental principle. Figure 10d illustrates the addition of 10% CR to concrete reinforced with 1.5% PVA fiber. This shows the crack bridging effect of the fiber, which reduces micropores and makes the concrete hard, resulting in the development of mechanical strength. Moreover, Fig. 10e illustrates the addition of 10% CR to concrete, blended with 2% PVA fiber. This blend demonstrates the clumping effect of the fiber, which increases the size of the pores and increases the water absorption of the concrete. This results in a reduced connection between the cement mortar and other ingredients of the CR concrete, thereby reducing its strength. Besides, Fig. 10f shows the higher content of CR included in concrete reinforced with 2% of PVA fiber. A higher CR may negatively impact it. The adverse effects of rubber particles on PVA fiber-blended concrete are caused by the hydrophobic properties of CR, which result in the development of regional areas with a reduced water–cement ratio. This reduces the connection between

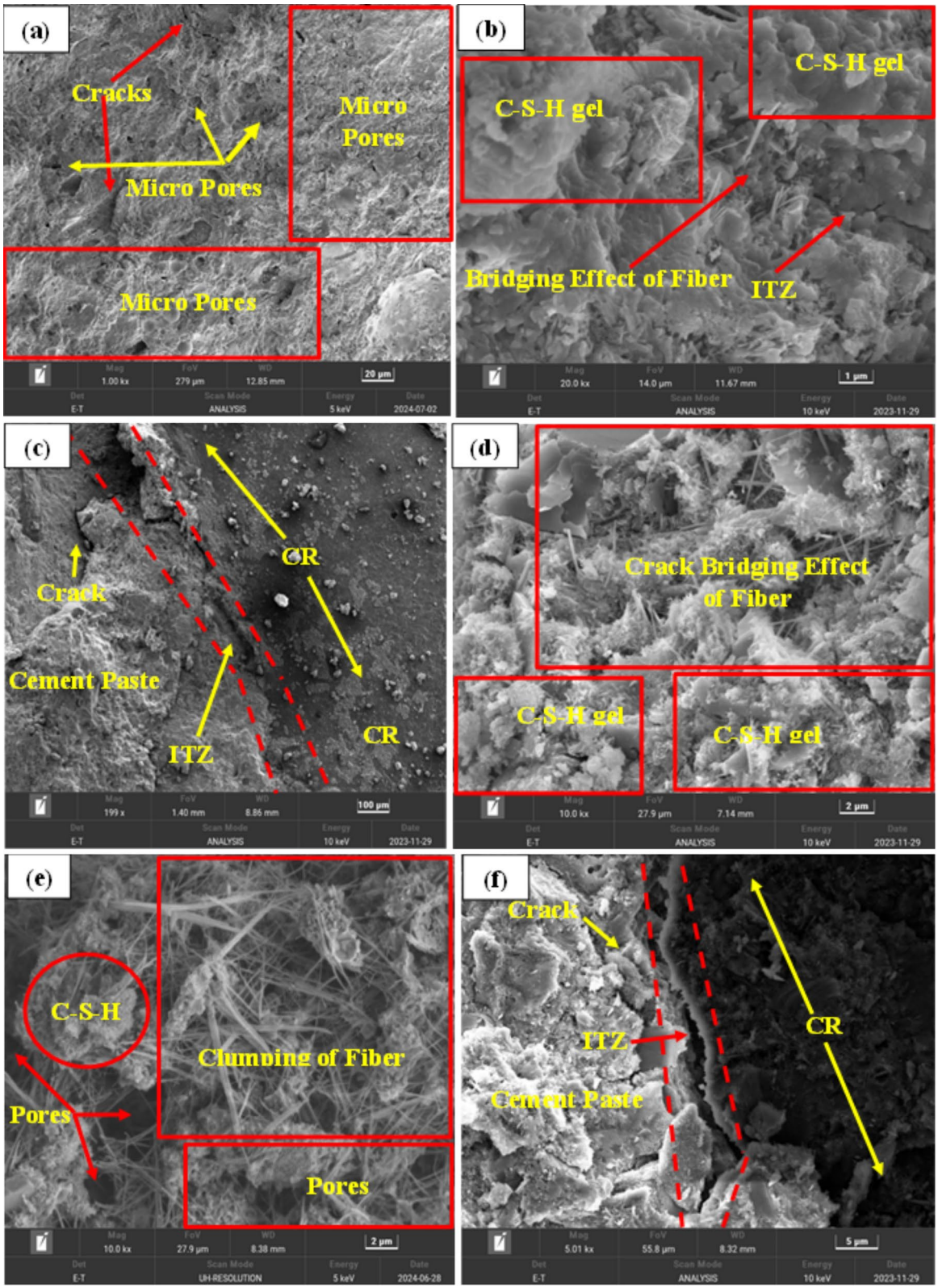

Fig. 10 Microstructural analysis of CR concrete for **a** M0 (control sample), **b** M1 (10% of CR, 1% PVA fiber), **c** M11 (30% of CR, 1% PVA fiber), **d** M2 (10% of CR, 1.5% PVA fiber), **e** M12 (10% of CR, 2% PVA fiber), and **f** M3 (30% of CR, 2% PVA fiber)

cement clinker and the solution responsible for pore formation, consequently decreasing the hydration process.

4 Sustainability assessment

4.1 Embodied carbon (EC)

This research conducted a sustainability evaluation for 13 various combinations to calculate the EC of rubberized concrete supplemented with different volumes of PVA fiber. The EC readings for all components of CR concrete were derived from previous studies, as presented in Table 4. Nevertheless, the amount of carbon dioxide (CO_2) emitted for any possible combination of rubberized concrete may be calculated using Eq. 1. In Eq. 1 (Bheel et al., 2021b), the signs CO_{2e}, i, and Wi denote the overall EC and the weight per unit volume (i.e., kg/m3) for each combination. In addition, the abbreviation CO_{2i} represents the EC of CR concrete elements, as shown in Table 4.

$$CO_{2e} = \sum_{i=1}^{n} (W_i \times CO_{2i}) \quad (1)$$

Figure 11 displays the outcomes of the CO_2 emissions produced from all combinations of rubberized concrete. All CR concrete combinations demonstrated greater CO_2 releases as compared to CM. Figure 11 illustrates the calculation of the EC of the CR combination at various levels of PVA fiber concentration. Figure 11 reveals that the PC has the highest carbon emissions, followed by PVA fiber, CA, CR, sand, and an SP. Nevertheless, the PVA fiber content plays an important role in the CR concrete, as seen in Fig. 11. Consequently, the addition of PVA fiber in the CR concrete leads to a boost in its EC. In addition, the substitution of a portion of the sand with CR also leads to an increase in the carbon dioxide greenhouse emissions of CR concrete. The main reason for this is the greater carbon dioxide releases of CR in comparison to sand, as seen in Table 4. In the case of CR, the CO_2 emissions arise from the fuel consumption associated with the grinding and reduction of discarded tires into smaller fragments, along with the transportation of these components. Nevertheless, CR does not generate any carbon dioxide emissions since it is derived only

Table 4 Embodied carbon of CR concrete blended with PVA fiber

Components	Embodied carbon ($kgCO_2/kg$)	References
PC	0.912	Zhu et al., 2022
Sand	0.0139	Turner & Collins, 2013
CR	0.06	Magnusson & Mácsik, 2017
PVA	3.60	Huang et al., 2013
CA	0.0408	Turner & Collins, 2013
Water	0	Yang et al., 2013
SP (HRWR)	1.48	Huang et al., 2013

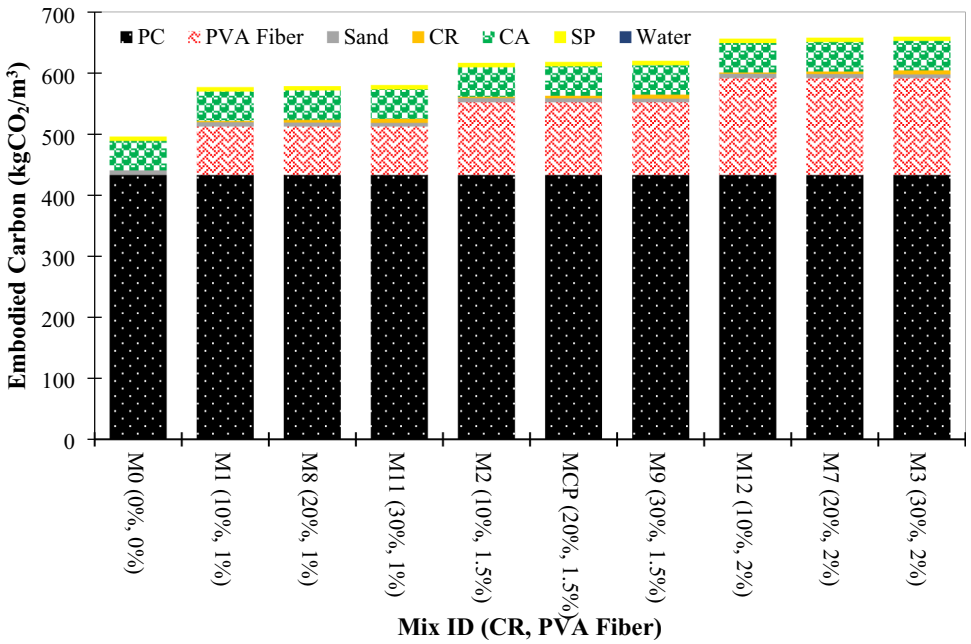

Fig. 11 Embodied carbon of rubberized concrete containing PVA fiber

from waste tires. The predicted EC values for concrete added with 10%, 20%, and 30% CR are 656.45 $kgCO_2/m^3$, 658.11 $kgCO_2/m^3$, and 659.78 kg CO_2/m^3, correspondingly, when 2% of PVA fiber is used. The combined utilization of PVA fiber and CR in concrete has been seen to result in a higher emission of EC in rubberized concrete. Bheel et al., (2023b) found that including PVA fiber in composites leads to an increase in EC. Adamu et al., (2018) stated that the utilization of sand replaced with CR increases in concrete that results in improving the EC.

4.2 Eco-strength efficiency (ESE)

In order to enhance understanding, Eq. 2 can be used to compute a measurement of eco-strength efficiency (Bheel et al., 2021b):

$$Eco-strength\ efficiency = \frac{Average\ 28-day\ compressive\ strength\ of\ concrete}{Total\ embodied\ carbon\ of\ concrete}. \quad (2)$$

The ESE of rubberized concrete is calculated via Eq. 2 at different concentrations of PVA fiber, as shown in Fig. 12. The ESE values for concrete reinforced with 10%, 20%, and 30% CR were determined to be 0.082 $MPa/kgCO_2/m^3$, 0.074 $MPa/kgCO_2/m^3$, and 0.065 $MPa/kgCO_2/m^3$, correspondingly, when 1% PVA fiber was added to rubberized concrete after 28 days. It has been shown that the ESE of CR concrete improves when the volume percentage of PVA fiber in the concrete decreases. The decrease in ESE may be attributed to the increase in PVA content, which leads to a rise in the presence of free gaps and porosity in concrete. Consequently, this drop in ESE is seen in rubberized concrete. The reason for this is that rubberized concrete has superior CS and the smallest amount of carbon while including 1% PVA fiber in the concrete compared to other mixtures. Bheel et al., (2023b) reported that the utilization of PVA fiber rises in composites that results in reducing the ESE. Furthermore, it can observe an overall reduction in ESE of concrete when the consumption of CR increases in concrete. This reduction can be due to the smooth surface texture of CR (Dong et al., 2013; Gupta et al., 2014; Meyyappan et al., 2023; Mohammed & Adamu, 2018) observed reduction in CS owing to rise in CR as more voids are produced by the addition of CR that results in reducing the ESE of concrete.

5 Optimization and modeling by response surface methodology (RSM)

5.1 ANOVA

The experimental data are used to develop and validate empirical response prediction approaches. Equations (3) and (4) for linear and quadratic relationships, correspondingly, illustrate how the input factors

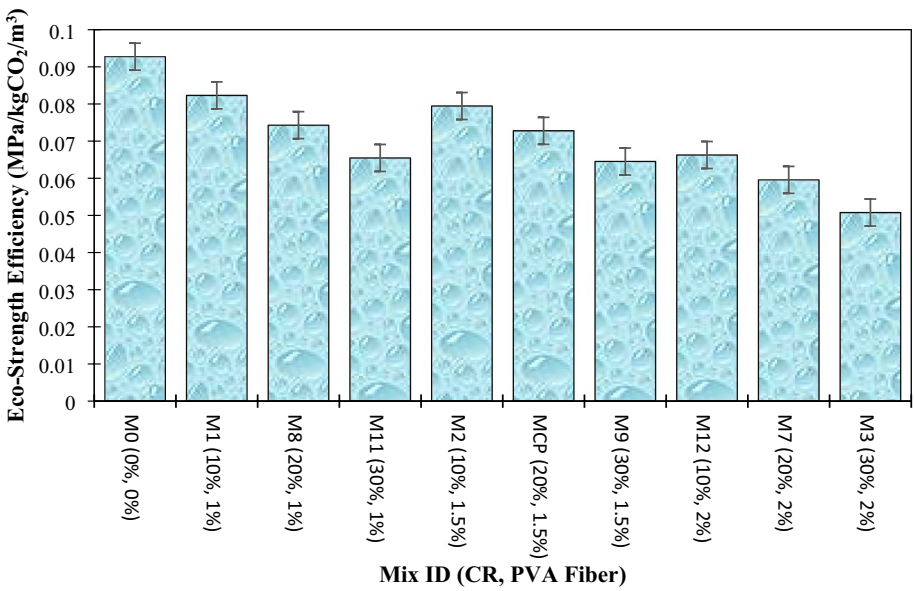

Fig. 12 ESE of rubberized concrete containing PVA fiber

interact and affect the desired response, which can be used to determine the form of the model:

$$y = \beta_0 + \beta_1 x_2 + \beta_2 x_2 + \beta_n x_n + \epsilon \tag{3}$$

$$y = \beta_0 + \sum_{i=1}^{k} \beta_i x_i + \sum_{i=1}^{k} \beta_{ii} x_i^2 + \sum_{j=2}^{k} \sum_{i=1}^{j=1} \beta_{ij} x_i x_j + \epsilon. \tag{4}$$

Equations 5–9 display the developed models. The quadratic approaches were observed to be more appropriate for the CS, TS, FS, WA, and DD of CR concrete, and the selection was made depending on the SMSS, prioritizing extra terms that are deemed important and ensuring that the model remains unaliased. Moreover, the input variables' minimum, mean, and maximum values are characterized by the codes − 1, 0 and + 1, respectively, in the models' depiction of the factors (Bheel et al., 2023c, 2023d, 2023e, 2023f):

$$\begin{aligned} CS = &+ 44.57 - 4.75 \times A - 2.05 \\ &\times B - 0.13 \times AB - 0.23 \\ &\times A^2 - 3.63 \times B^2, \end{aligned} \tag{5}$$

$$\begin{aligned} TS = &+ 3.93 - 0.42 \times A - 0.18 \\ &\times B - 0.011 \times AB - 0.020 \\ &\times A^2 - 0.32 \times B^2, \end{aligned} \tag{6}$$

$$\begin{aligned} FS = &+ 5.35 - 0.57 \times A - 0.25 \\ &\times B - 0.015 \times AB - 0.028 \\ &\times A^2 - 0.44 \times B^2, \end{aligned} \tag{7}$$

$$\begin{aligned} DD = &+ 1786.10 - 255.83 \times A - 96.50 \\ &\times B + 7.75 \times AB + 33.64 \\ &\times A^2 + 1.64 \times B^2, \end{aligned} \tag{8}$$

$$\begin{aligned} WA = &+ 3.45 + 0.37 \times A + 0.28 \\ &\times B + 0.058 \times AB + 0.099 \\ &\times A^2 - 0.036 \times B^2, \end{aligned} \tag{9}$$

where B is the PVA fiber and A is the CR addition through sand replacement. ANOVA was conducted on the models, utilizing a 95 percent confidence interval. Consequently, terms and models having a probability of less than five percent were deemed significant. Table 5 presents a summary of the ANOVA result. Because each of the developed models has a possibility value smaller than 0.005, they are all considered significant (Abdulkadir et al., 2024a, 2024b; Bheel & Mohammed, 2024; Udeze et al., 2024). As indicated in Table 5, the prototype terms are categorized as important or not important founded on whether the term's p-value greater than F value is, in that case, smaller or greater than 5 percent. On the other hand, the significance threshold for lack of fit must be less than 5% for the model to fit adequately. As a result, the only two approaches with a notable lack of fit among all those created are the DD and WA models. But when we look at other diagnostic tool models, even the WA and DD models prove to be effective enough for the intended use.

Table 6 also contains a list of additional model validation parameters that were taken into account during the analysis. As can be seen, the developed model's fit to the empirical data is gauged by its coefficient of determination (R^2), which is comparatively high for all models. A value of 1 or very near to 1 is the most desirable for R^2, which has a range of 0 to 1 (or 0 to 100 percent). All of the models had R^2 values between 98 and 99 percent, which suggests that the models that were chosen fit the data quite well. Furthermore, in order for the model to accurately predict the response, there should be no difference between the adjusted R^2 and the predicted R^2 greater than 0 points. Observing the Adj. values. Pred and R^2. Every model's R^2 indicates that this requirement is satisfied. Furthermore, a developed model needs to have a respectable level of precision (Adeq. Precision) of greater than four, and in this instance, an Adeq is present in every developed model. A model's strength and ability to predict responses accurately are demonstrated by an accuracy greater than 10.

5.2 Model diagnostics and response surface plots

In response surface methodology, one of the diagnostic apparatuses intended to measure the level of accuracy of a produced framework is the actual vs. projected diagram, which compares the model's efficacy with the null model. For a good fit, the data points should align with the 45-degree fit line with narrow confidence bands. On the other hand, a 2D chart or a 3D diagram can be used to more clearly visualize the outcome of the variables' interaction on the response. The identical data in 2D charts are expressed in a 3D manner by the 3D response surface plot. In this investigation, the real vs. Figures 13, 14, 15, 16 and 17 display the 3D response surface plots and the predicted diagnostic plot for each developed response prediction model. The predicted against actual charts demonstrate a strong relationship between the investigational information and the predicted outcome information from models, as can be seen by the fact that all of the developed models' data points are exactly aligned with the fitted line.

Color coding is used to identify areas on the 3D response surface plots that correspond to various response intensities that can be achieved by interacting

Table 5 The outcome of the ANOVA

Response	Source	Sum of squares	Df	Mean square	F-value	p-value > F	Significance
CS	Model	204.44	5	41.08	118.31	< 0.0002	Important
	A-CR	133.39	1	135.39	394.12	< 0.0002	Important
	B-PVA	26.21	1	25.21	71.23	< 0.0002	Important
	AB	0.064	1	0.064	0.19	0.6828	Not important
	A^2	0.14	1	0.16	0.41	0.5367	Not important
	B^2	36.39	1	36.39	105.65	< 0.0001	Important
	Residual	2.42	7	0.35			
	Lack of fit	0.40	3	0.13	0.26	0.8421	Not important
	Pure error	2.01	4	0.51			
	Cor total	207.85	12				
FS	Model	2.97	5	0.58	118.31	< 0.0002	Important
	A-CR	1.96	1	1.94	394.12	< 0.0002	Important
	B-PVA	0.37	1	0.37	71.25	< 0.0002	Important
	AB	9.001E-004	1	9.001E-004	0.19	0.6828	Not important
	A^2	2.092E-003	1	2.092E-003	0.43	0.5367	Not important
	B^2	0.51	1	0.53	105.64	< 0.0002	Important
	Residual	0.034	7	4.958E-004			
	Lack of fit	5.912E-003	3	1.972E-004	0.28	0.8421	Not important
	Pure error	0.028	4	7.201E-004			
	Cor total	2.98	12				
TS	Model	1.60	5	0.31	118.31	< 0.0002	Important
	A-CR	1.10	1	1.07	394.12	< 0.0002	Important
	B-PVA	0.25	1	0.19	71.25	< 0.0002	Important
	AB	4.841E-004	1	4.841E-004	0.19	0.6828	Not important
	A^2	1.126E-003	1	1.126E-003	0.43	0.5367	Not important
	B^2	0.29	1	0.27	105.65	< 0.0002	Important
	Residual	0.018	7	2.666E-003			
	Lack of fit	3.181E-003	3	1.061E-003	0.28	0.8421	Not important
	Pure error	0.016	4	3.871E-003			
	Cor total	1.62	12				
DD	Model	4.527E + 005	5	90,524.57	472.48	< 0.0001	Important
	A-CR	3.928E + 005	1	3.928E + 005	2049.5	< 0.0001	Important
	B-PVA	55,874.50	1	55,874.50	290.61	< 0.0001	Important
	AB	241.25	1	241.25	1.26	0.2997	Important
	A^2	3124.12	1	3125.11	16.32	0.0048	Important
	B^2	7.42	1	7.42	0.038	0.8498	Not important
	Residual	1342.22	7	191.61			
	Lack of fit	1335.42	3	445.47	370.23	< 0.0001	Important
	Pure error	4.81	4	1.23			
	Cor total	4.541E + 005	12				

Table 5 (continued)

Response	Source	Sum of squares	Df	Mean square	F-value	p-value > F	Significance
WA	Model	1.31	5	0.25	98.23	< 0.0001	Important
	A-CR	0.82	1	0.83	304.92	< 0.0001	Important
	B-PVA	0.48	1	0.48	177.20	< 0.0001	Important
	AB	0.014	1	0.014	4.96	0.0613	Not important
	A^2	0.028	1	0.028	10.11	0.0154	Not important
	B^2	3.623E-003	1	3.623E-004	1.37	0.2824	Important
	Residual	0.018	7	2.660E-004			
	Lack of fit	0.019	3	5.924E-004	25.74	0.0046	Important
	Pure error	9.201E-004	4	2.301E-005			
	Cor total	1.35	12				

Table 6 Validation parameters

Model validation constraints	CS	TS	FS	DD	PR
Std. Dev	0.59	0.052	0.070	13.84	0.052
Mean	42.78	3.77	5.13	1802.38	3.48
C.V. %	1.37	1.37	1.37	0.77	1.49
PRESS	6.58	0.051	0.095	12,726.70	0.18
-2 log likelihood	14.99	− 48.20	− 40.14	97.17	− 48.19
R-squared	0.9884	0.9884	0.9884	0.9970	0.9861
Adj R-squared	0.9801	0.9801	0.9801	0.9949	0.9762
Pred R-squared	0.9684	0.9684	0.9684	0.9720	0.8655
Adeq precision	38.388	38.388	38.388	74.934	36.940
BIC	30.38	− 32.81	− 24.75	112.56	− 32.80
AICc	40.99	− 22.20	− 14.14	123.17	− 22.19

with the input variables. The blue zones show the lowest response intensities, and the red regions indicate the areas with the most intense responses level. As demonstrated by the graphs, the interactions between the input factors and how they affect the responses are entirely reliable with the prior discussions on how the variables affect the mechanical properties of the rubberized concrete.

5.3 Multiple objective optimization

The goal of optimization is to generate the intended result at the best possible variable counts. Goals with varying conditions and significance levels are established for parameters (input and output factors) in order to achieve the intended purpose. The optimization is assessed using the desirability value, which ranges from 0 to 1. The value is closer to one the better the outcome. In this instance, Table 7 displays the results as well as the objective functions of the optimization. The outcome demonstrates that an ideal CS, TS, FS, DD, and WA of 44.30 MPa, 3.898 MPa, 5.316 percent, and 1774.87 kg/m3 could be produced with optimal input factors of 20.099 percent CR and 1.545 percent PVA fiber additions, and with a high desirability value of 60.80 percent, 3.479 percent. The desirability results are displayed in Figs. 18.

5.4 Experimental validation

The last stage of the RSM analysis entails generating samples with the suggested optimized input variables in order to validate the developed approaches experimentally and the optimization outcomes. The samples were tested experimentally and optimization predictions were compared after 28 days of curing. Equation 10 (Bheel et al., 2024) was applied to calculate the experimental error, and Table 8 displays the results. It is evident that, for every response, there was less than a 10% percentage error between the investigational outcomes and predicted outcomes. Consequently, it is possible to predict the answers with a high degree of accuracy using the developed Eqs. (5–9):

$$\delta = \left| \frac{\vartheta_E - \vartheta_P}{\vartheta_P} \right| \times 100\%. \tag{10}$$

6 Conclusions

This study included testing CR concrete with different volumes of PVA fiber to examine its mechanical and physical qualities. According to the scientific findings and findings gathered, the following assumptions might be determined:

- When compared to the standard mix, the M2 mix containing 10% rubber crumbs and 1% PVA fibers had the highest CS; however, after 7, 14, and

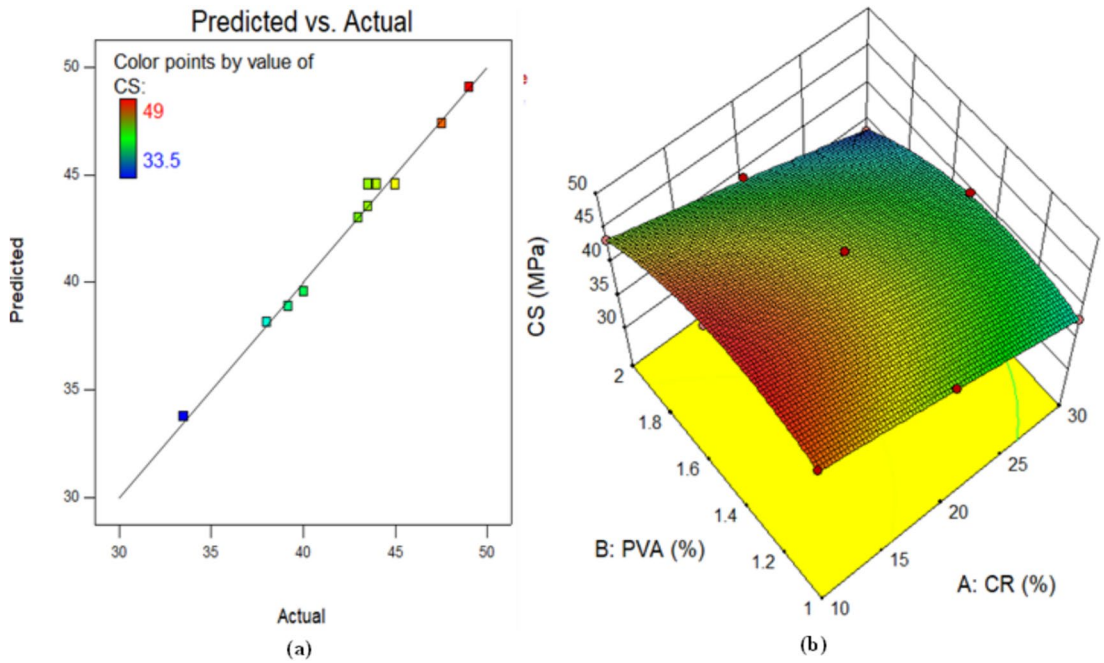

Fig. 13 **a** Predicted against actual plots, **b** 3D figure for CS of rubberized concrete

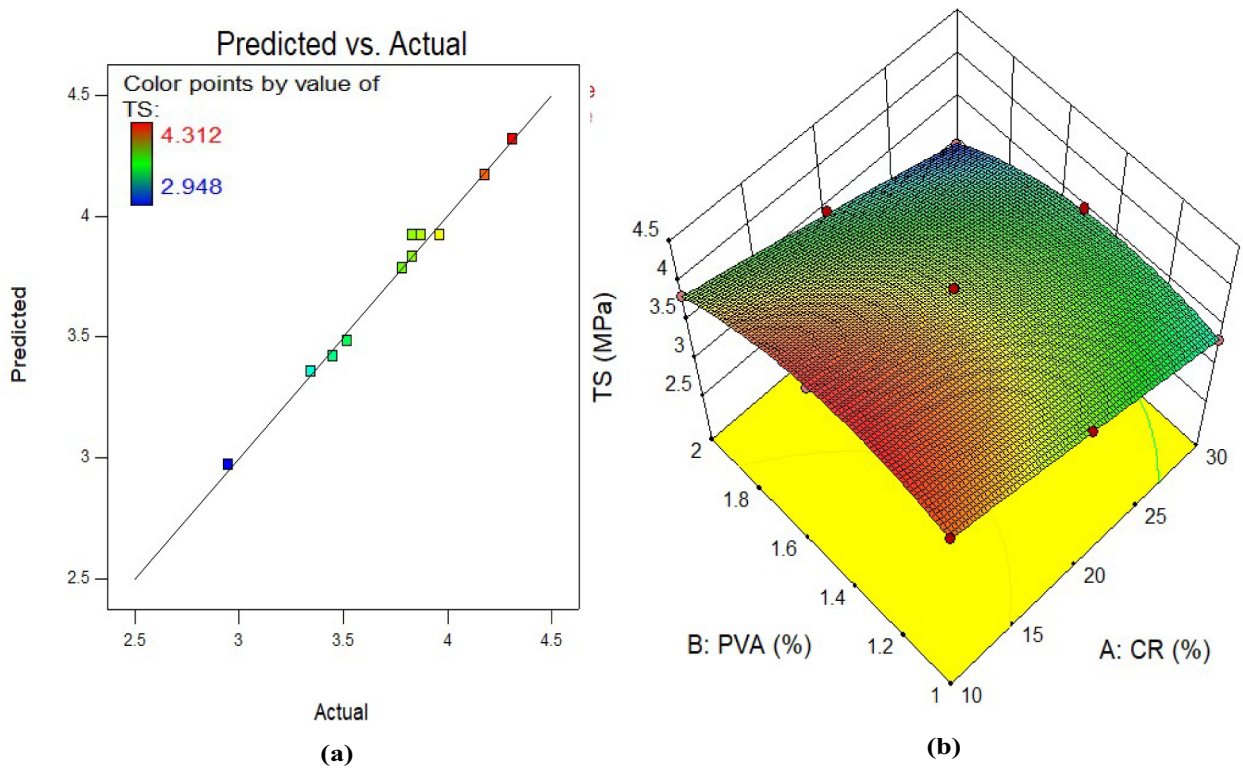

Fig. 14 **a** Predicted against actual plots, **b** 3D figure for TS of rubberized concrete

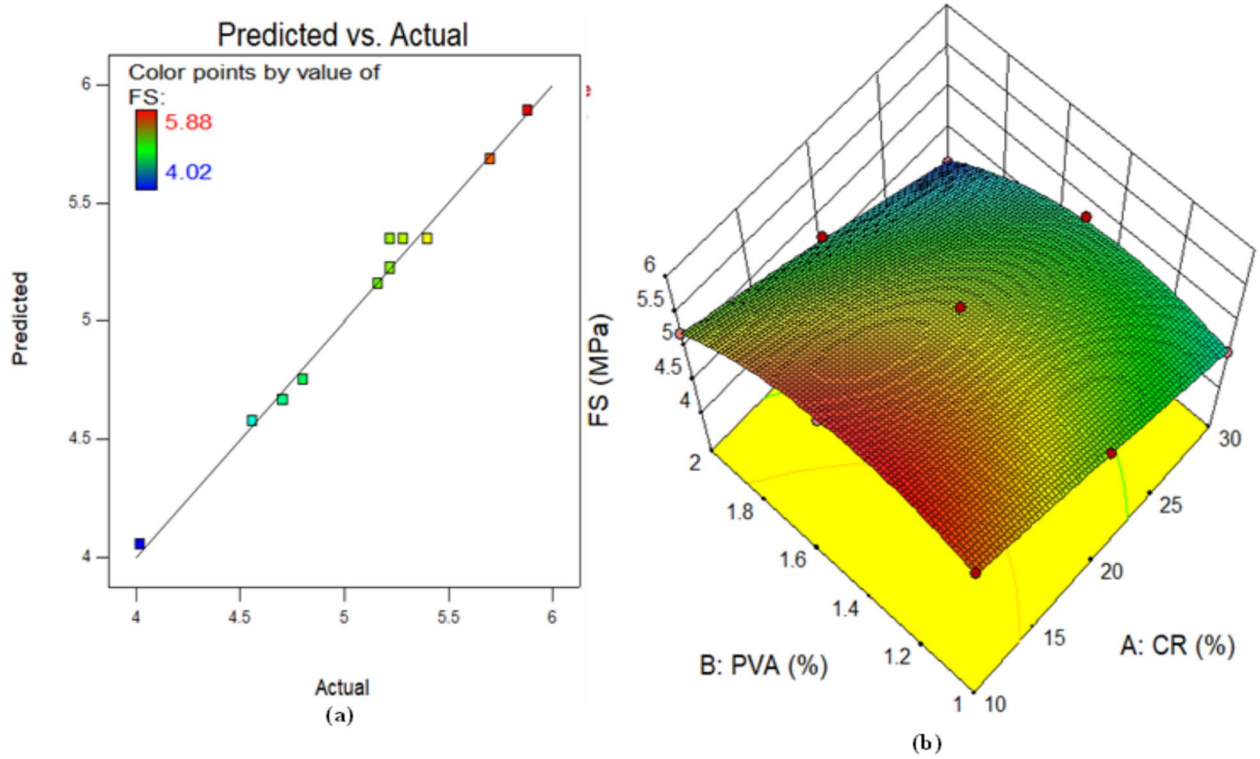

Fig. 15 **a** Predicted against actual plots, **b** 3D figure for FS of rubberized concrete

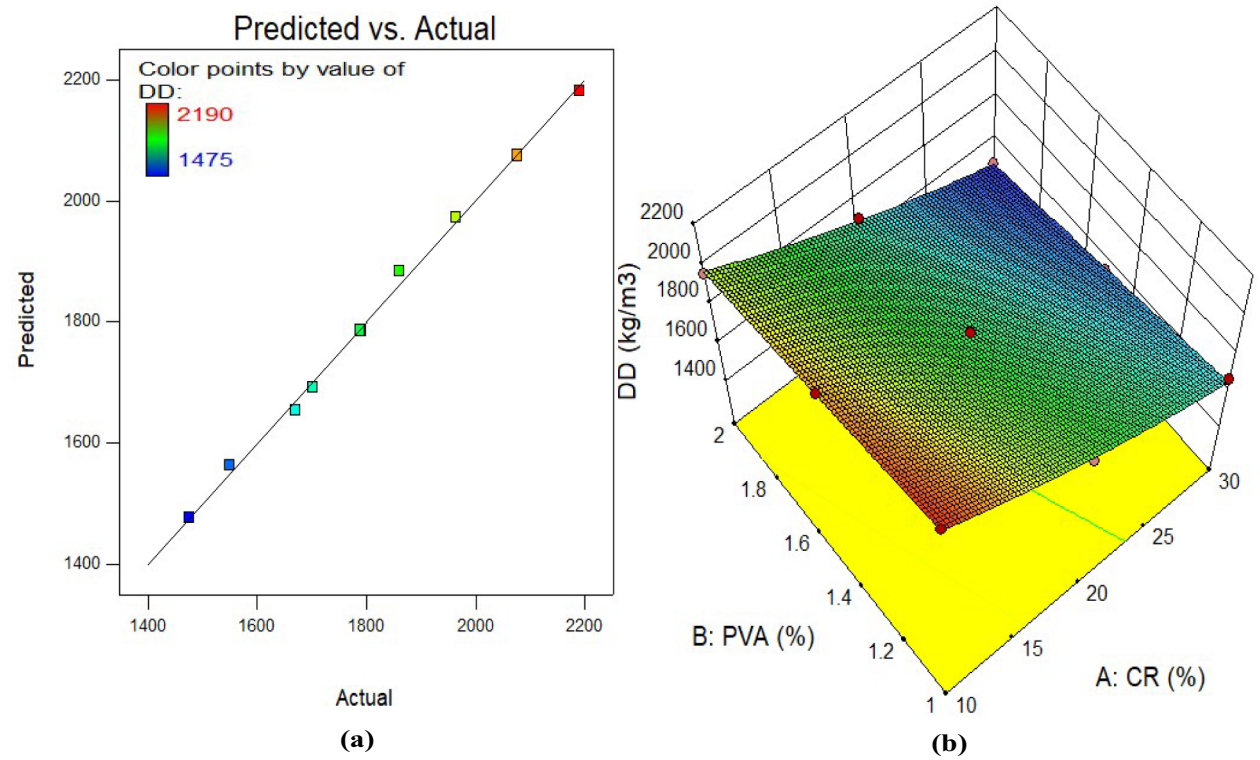

Fig. 16 **a** Predicted against actual plots, **b** 3D figure for DD of rubberized concrete

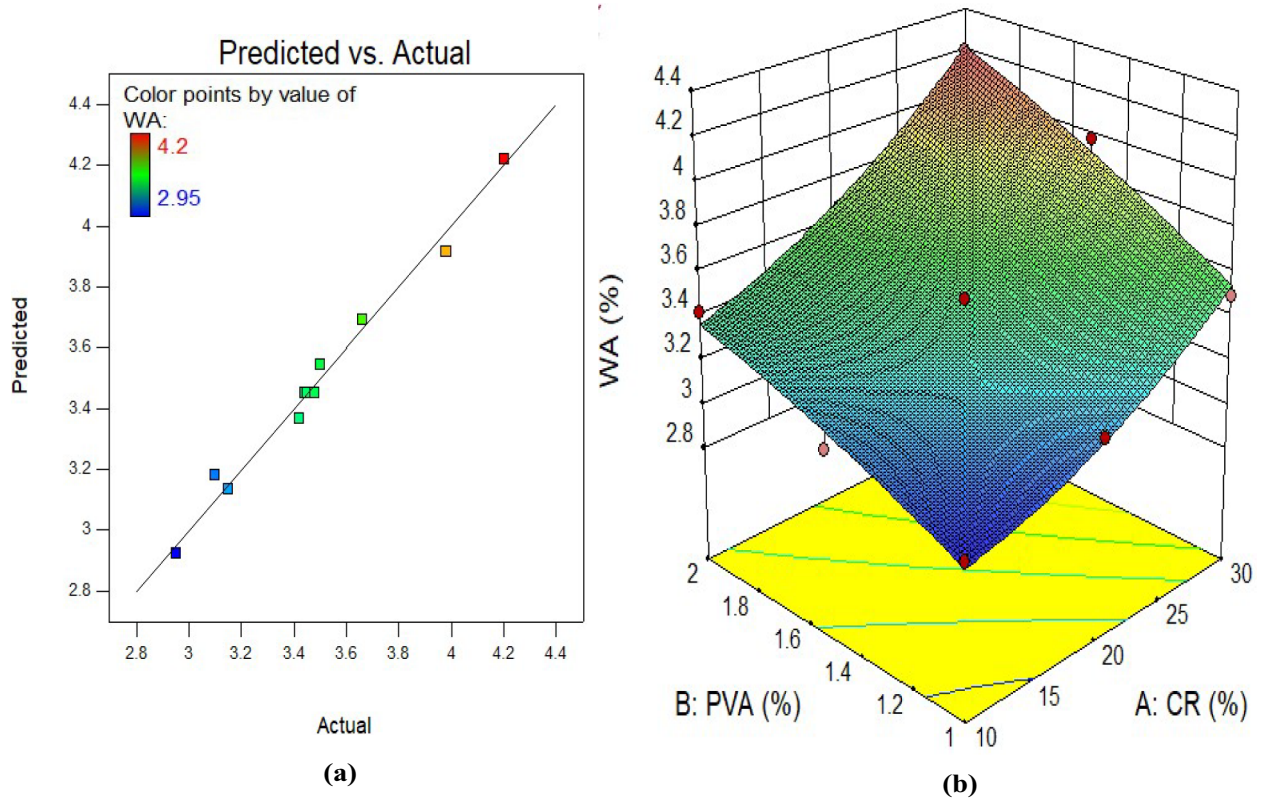

Fig. 17 **a** Predicted against actual plots, **b** 3D figure for WA of rubberized concrete

Table 7 Criteria and solutions for multi-objective optimization

Factors		Input factors (%)		Responses (output factors)				
		CR (%)	PVA (%)	CS (MPa)	TS (MPa)	FS (MPa)	DD (kg/m^3)	WA (%)
Value	Minimum	10	1	33.50	2.948	4.02	1475	2.95
	Maximum	20	2	49	4.312	5.88	2190	4.20
Goal		In range	In range	Maximum	Maximum	Maximum	Minimum	Maximum
Result		20.099	1.545	44.30	3.898	5.316	1774.87	3.479
Desirability		0.608 (60.80%)						

28 days of curing, the CS of the other mix combinations decreased.

- Optimum tensile strength is observed in a concrete mix containing 10% rubber crumbs and 1.5% PVA fibers, with the increase in rubber and fibers it was seen in the reduction in TS.
- Flexural strength is maximum in a concrete mix having 10% rubber crumbs and 1.5% PVA fibers followed by 10% rubber crumbs and 1% PVA fibers and thereby reduction in the flexural strength for other combinations due to improper bond between rubber and mortar for increased rubber content.
- Concrete with 30% rubber crumbs and 2% PVA fibers has maximum water absorption and water absorption decreases as the percentage of rubber and fibers is decreased, hence voids and airspaces are avoided due to proper compaction.
- As rubber and fiber content rises, the mix with 30% rubber crumb and 2% PVA fiber has the lowest DD and the mix with the highest DD is the normal mix. Rubber and fiber densities are the lowest in relation to the other constituents in mixture, the DD of the CR concrete decreases.

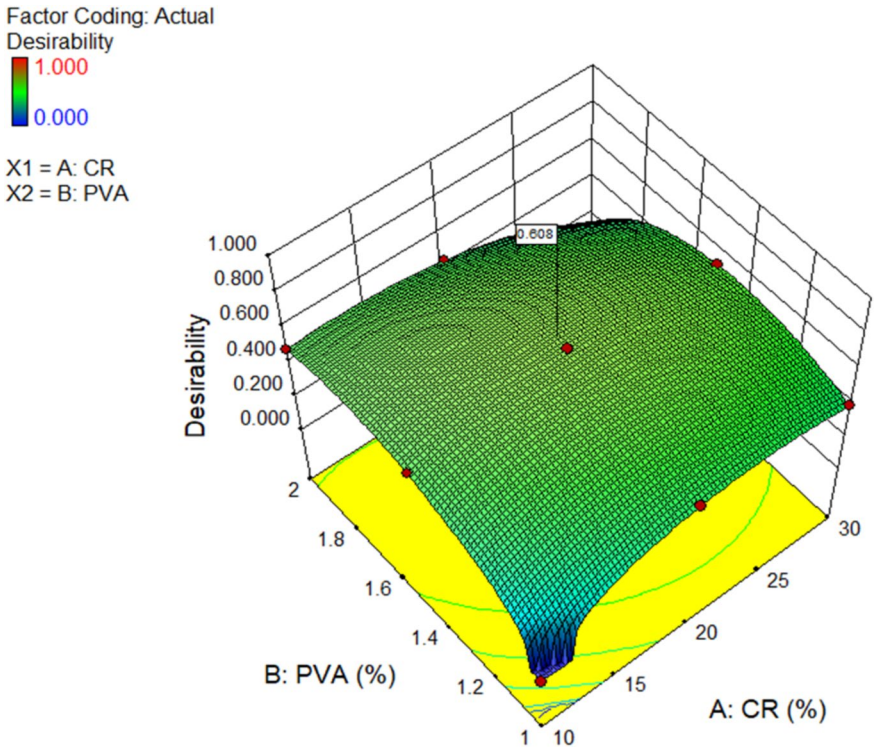

Fig. 18 3D plot of desirability factor of the study

Table 8 Validation with experimentation

Response	Investigational outcome	Predicted outcome	Error (%)
CS (MPa)	45.20	44.308	2.01
TS (MPa)	3.97	3.899	1.82
FS (MPa)	5.50	5.317	3.44
DD (kg/m^3)	1752	1775.14	1.30
WA (%)	3.53	3.478	1.50

- The increase in the quantity of PVA fiber and CR in concrete leads to an augmentation in the EC. The combined application of PVA fiber and CR has been noted to enhance the rubberized concrete, leading to a drop in ESC.
- The microstructural characteristics of CR concrete combined with numerous contents of PVA fiber were analyzed. The integration of CR in concrete that results in enhancing the micro-pores which reduces the strength of concrete while the PVA fiber reduces the micro-pores and increases the mechanical characteristics up to certain level.
- It has been spotted that the utilization of 1% PVA fiber offers highest findings of concrete blended with 10% of CR as substitution for sand, therefore it is suggested for construction purpose.

Acknowledgements
NA

Author contributions
NB (software, lab work, analysis, writing the first draft), AVB (methodology, lab work, analysis, writing the paper) AND BSM (supervision, concept, reviewing and editing, funding).

Funding
The authors express their gratitude to Universiti Teknologi PETRONAS, Malaysia, for providing the funding to conduct this study under the grant numbers 015ME0-238 and 015ME0-284.

Availability of data and materials
The datasets used and/or analyzed during the current study are available from the corresponding author on reasonable request.

Declarations

Competing interests
The authors declare that they have no competing interests.

Received: 6 May 2024 Accepted: 3 November 2024
Published online: 23 January 2025

References

Abdulkadir, I., Mohammed, B. S., Ali, M. O. A., & Liew, M. S. (2022). Effects of graphene oxide and crumb rubber on the fresh properties of self-compacting engineered cementitious composite using response surface methodology. *Materials*. https://doi.org/10.3390/ma15072519

Abdulkadir, I., Mohammed, B. S., Al-Yacouby, A. M., Woen, E. L., & Tafsirojjaman, T. (2024b). Tailoring an engineered cementitious composite with enhanced mechanical performance at ambient and elevated temperatures using graphene oxide and crumb rubber. *Journal of Materials Research and Technology, 28*, 4508–4530. https://doi.org/10.1016/j.jmrt.2024.01.059

Abdulkadir, I., Mohammed, B. S., Liew, M. S., & Wahab, M. M. A. (2021a). Modelling and optimization of the mechanical properties of engineered cementitious composite containing crumb rubber pretreated with graphene oxide using response surface methodology. *Construction and Building Materials*. https://doi.org/10.1016/j.conbuildmat.2021.125259

Abdulkadir, I., Mohammed, B. S., Liew, M. S., & Wahab, M. M. A. (2021b). Modelling and optimization of the impact resistance of graphene oxide modified crumb rubber-ECC using response surface methodology. *IOP Conference Series: Materials Science and Engineering*. https://doi.org/10.1088/1757-899x/1197/1/012043

Abdulkadir, I., Mohammed, B. S., Woen, E. L., Sing, W. L., & Al-Yacouby, A. M. (2024a). Optimizing sulfate and acid resistance in rubberized engineered cementitious composite with graphene oxide-pretreated crumb rubber: A response surface methodology approach. *Developments in the Built Environment*. https://doi.org/10.1016/j.dibe.2024.100405

Abdullah, G. M. S., Chohan, I. M., Ali, M., Bheel, N., Ahmad, M., Najeh, T., Gamil, Y., & Almujibah, H. R. (2024). Effect of titanium dioxide as nanomaterials on mechanical and durability properties of rubberised concrete by applying RSM modelling and optimizations. *Frontiers in Materials*. https://doi.org/10.3389/fmats.2024.1357094

Adamu, M., Mohammed, B. S., & Shahir Liew, M. (2018). Mechanical properties and performance of high volume fly ash roller compacted concrete containing crumb rubber and nano silica. *Construction and Building Materials, 171*, 521–538. https://doi.org/10.1016/j.conbuildmat.2018.03.138

Aghamohammadi, O., Mostofinejad, D., Mostafaei, H., & Abtahi, S. M. (2024). Mechanical properties and impact resistance of concrete pavement containing crumb rubber. *International Journal of Geomechanics*. https://doi.org/10.1061/ijgnai.gmeng-7620

Al-Fakih, A., Wahab, M. M. A., Mohammed, B. S., Liew, M. S., Abdullah Zawawi, N. A. W., & Asad, S. (2020). Experimental study on axial compressive behavior of rubberized interlocking masonry walls. *Journal of Building Engineering*. https://doi.org/10.1016/j.jobe.2019.101107

Al-Hadithi, A. I., Noaman, A. T., & Mosleh, W. K. (2019). Mechanical properties and impact behavior of PET fiber reinforced self-compacting concrete (SCC). *Composite Structures*. https://doi.org/10.1016/j.compstruct.2019.111021

Alhozaimy, A. M., Soroushian, P., & Mirza, F. (1996). Mechanical properties of polypropylene fiber reinforced concrete and the effects of pozzolanic materials. *Cement and Concrete Composites, 18*, 85–92. https://doi.org/10.1016/0958-9465(95)00003-8

Alwi Assaggaf, R., Uthman Al-Dulaijan, S., Maslehuddin, M., Baghabra Al-Amoudi, O. S., Ahmad, S., & Ibrahim, M. (2022). Effect of different treatments of crumb rubber on the durability characteristics of rubberized concrete. *Construction and Building Materials*. https://doi.org/10.1016/j.conbuildmat.2021.126030

Anas, M., Khan, M., Bilal, H., Jadoon, S., & Khan, M. N. (2022). Fiber reinforced concrete: A review †. *Engineering Proceedings*. https://doi.org/10.3390/engproc2022022003

Aslani, F., Ma, G., Yim Wan, D. L., & Muselin, G. (2018). Development of high-performance self-compacting concrete using waste recycled concrete aggregates and rubber granules. *Journal of Cleaner Production, 182*, 553–566. https://doi.org/10.1016/j.jclepro.2018.02.074

ASTM C150/C150M-16e1, (2016) Specification for Portland Cement, ASTM International, West Conshohocken, PA, 2016

Batayneh, M. K., Marie, I., & Asi, I. (2008). Promoting the use of crumb rubber concrete in developing countries. *Waste Management, 28*, 2171–2176. https://doi.org/10.1016/j.wasman.2007.09.035

Benazzouk, A., Douzane, O., Langlet, T., Mezreb, K., Roucoult, J. M., & Quéneudec, M. (2007). Physico-mechanical properties and water absorption of cement composite containing shredded rubber wastes. *Cement and Concrete Composites, 29*, 732–740. https://doi.org/10.1016/j.cemconcomp.2007.07.001

Bheel, N., Ali, M. O. A., Kırgız, M. S., Shafiq, N., & Gobinath, R. (2023a). Effect of graphene oxide particle as nanomaterial in the production of engineered cementitious composites including superplasticizer, fly ash, and polyvinyl alcohol fiber. *Materials Today: Proceedings*. https://doi.org/10.1016/j.matpr.2023.03.010

Bheel, N., Ali, M. O. A., Liu, Y., Tafsirojjaman, T., Awoyera, P., Sor, N. H., & Romero, L. M. B. (2021b). Utilization of corn cob ash as fine aggregate and ground granulated blast furnace slag as cementitious material in concrete. *Buildings*. https://doi.org/10.3390/buildings11090422

Bheel, N., & Mohammed, B. S. (2024). Modelling and optimization of long-term modulus of elasticity and Poisson's ratio of graphene oxide based engineered cementitious composites by using response surface methodology. *Diamond and Related Materials*. https://doi.org/10.1016/j.diamond.2024.110949

Bheel, N., Mohammed, B. S., Abdulkadir, I., Liew, M. S., & Zawawi, N. A. W. A. (2023f). Effects of graphene oxide on the properties of engineered cementitious composites: Multi-objective optimization technique using RSM. *Buildings*. https://doi.org/10.3390/buildings13082018

Bheel, N., Mohammed, B. S., Ahmed Ali, M. O., Shafiq, N., Mohamed Tag-eldin, E., & Ahmad, M. (2023b). Effect of polyvinyl alcohol fiber on the mechanical properties and embodied carbon of engineered cementitious composites. *Results in Engineering*. https://doi.org/10.1016/j.rineng.2023.101458

Bheel, N., Mohammed, B. S., Ali, M. O. A., Shafiq, N., & Radu, D. (2023c). Effect of graphene oxide as a nanomaterial on the bond behaviour of engineered cementitious composites by applying RSM modelling and optimization. *Jjournal of Materials Research and Technology, 26*, 1484–1507. https://doi.org/10.1016/j.jmrt.2023.07.278

Bheel, N., Mohammed, B. S., Liew, M. S., & Zawawi, N. A. W. A. (2023d). Effect of graphene oxide as a nanomaterial on the durability behaviors of engineered cementitious composites by applying RSM modelling and optimization. *Buildings*. https://doi.org/10.3390/buildings13082026

Bheel, N., Mohammed, B. S., Liew, M. S., & Zawawi, N. A. W. A. (2023e). Durability behaviours of engineered cementitious composites blended with carbon nanotubes against sulphate and acid attacks by applying RSM modelling and optimization. *Buildings*. https://doi.org/10.3390/buildings13082032

Bheel, N., Mohammed, B. S., Mohamad, H., Sutanto, M. H., & Tafsirojjaman, T. (2024). Synergetic effect of multiwalled carbon nanotubes on mechanical and deformation properties of engineered cementitious composites: RSM modelling and optimization. *Diamond and Related Materials*. https://doi.org/10.1016/j.diamond.2024.111299

Bheel, N., Tafsirojjaman, T., Liu, Y., Awoyera, P., Kumar, A., & Keerio, M. A. (2021a). Experimental study on engineering properties of cement concrete reinforced with nylon and jute fibers. *Buildings*. https://doi.org/10.3390/buildings11100454

Bing, C., & Ning, L. (2014). Experimental research on properties of fresh and hardened rubberized concrete. *Journal of Materials in Civil Engineering*. https://doi.org/10.1061/(asce)mt.1943-5533.0000923

Bisht, K., & Ramana, P. V. (2017). Evaluation of mechanical and durability properties of crumb rubber concrete. *Construction and Building Materials, 155*, 811–817. https://doi.org/10.1016/j.conbuildmat.2017.08.131

British Standards Institution, BS EN 12390–7:2000 (2000) Part 7: Density of hardened concrete, 389

BS EN 12390-3, (2009) Testing Harden Concrete. Compressive Strength of Test Specimens, BSI, London, UK.

BS EN 12390–5 (2009) Testing hardened concrete: flexural strength of test specimens. BSI. British Standard Institute.

BS 1881: Part 122 : 1983 Part 122. (n.d.) Method for determination of water absorption

Chen, A., Han, X., Chen, M., Wang, X., Wang, Z., & Guo, T. (2020). Mechanical and stress-strain behavior of basalt fiber reinforced rubberized recycled coarse aggregate concrete. *Construction and Building Materials*. https://doi.org/10.1016/j.conbuildmat.2020.119888

Dehdezi, P. K., Erdem, S., & Blankson, M. A. (2015). Physico-mechanical, microstructural and dynamic properties of newly developed artificial fly ash based lightweight aggregate—Rubber concrete composite. *Composites. Part B, Engineering, 79*, 451–455. https://doi.org/10.1016/j.compositesb.2015.05.005

Dong, Q., Huang, B., & Shu, X. (2013). Rubber modified concrete improved by chemically active coating and silane coupling agent. *Construction and Building Materials, 48*, 116–123. https://doi.org/10.1016/j.conbuildmat.2013.06.072

Eisa, A. S., Elshazli, M. T., & Nawar, M. T. (2020). Experimental investigation on the effect of using crumb rubber and steel fibers on the structural behavior of reinforced concrete beams. *Construction and Building Materials*. https://doi.org/10.1016/j.conbuildmat.2020.119078

El Naggar, H., & Abdo, A. M. A. (2023). Properties and behavior of rubberized concrete enhanced with PVA fibers. *Buildings, 13*(7), 1681. https://doi.org/10.3390/buildings13071681

Gesoğlu, M., Güneyisi, E., Khoshnaw, G., & Ipek, S. (2014). Abrasion and freezing-thawing resistance of pervious concretes containing waste rubbers. *Construction and Building Materials, 73*, 19–24. https://doi.org/10.1016/j.conbuildmat.2014.09.047

Gheni, A. A., ElGawady, M. A., & Myers, J. J. (2017). Mechanical characterization of concrete masonry units manufactured with crumb rubber aggregate. *ACI Materials Journal, 114*, 65–76. https://doi.org/10.14359/51689482

Girskas, G., & Nagrockienė, D. (2017). Crushed rubber waste impact of concrete basic properties. *Construction and Building Materials, 140*, 36–42. https://doi.org/10.1016/j.conbuildmat.2017.02.107

Gonen, T. (2018). Freezing-thawing and impact resistance of concretes containing waste crumb rubbers. *Construction and Building Materials, 177*, 436–442. https://doi.org/10.1016/j.conbuildmat.2018.05.105

Gupta, T., Chaudhary, S., & Sharma, R. K. (2014). Assessment of mechanical and durability properties of concrete containing waste rubber tire as fine aggregate. *Construction and Building Materials, 73*, 562–574. https://doi.org/10.1016/j.conbuildmat.2014.09.102

Hesami, S., Salehi Hikouei, I., & Emadi, S. A. A. (2016). Mechanical behavior of self-compacting concrete pavements incorporating recycled tire rubber crumb and reinforced with polypropylene fiber. *Journal of Cleaner Production, 133*, 228–234. https://doi.org/10.1016/j.jclepro.2016.04.079

Hossain, F. M. Z., Shahjalal, M., Islam, K., Tiznobaik, M., & Alam, M. S. (2019). Mechanical properties of recycled aggregate concrete containing crumb rubber and polypropylene fiber. *Construction and Building Materials, 225*, 983–996. https://doi.org/10.1016/j.conbuildmat.2019.07.245

Huang, X., Ranade, R., & Li, V. C. (2013). Feasibility study of developing green ECC using iron ore tailings powder as cement replacement. *Journal of Materials in Civil Engineering, 25*, 923–931. https://doi.org/10.1061/(asce)mt.1943-5533.0000674

Ismail, M. K., & Hassan, A. A. A. (2016). Performance of full-scale self-consolidating rubberized concrete beams in flexure. *ACI Materials Journal, 113*, 207–218. https://doi.org/10.14359/51688640

Japan Society of Civil Engineers. (2008). Recommendations for design and construction of high performance fiber reinforced cement composites with multiple fine cracks (HPFRCC). *Concrete Engineers Series, 82*, 6–10.

Jo, M., Soto, L., Arocho, M., St John, J., & Hwang, S. (2015). Optimum mix design of fly ash geopolymer paste and its use in pervious concrete for removal of fecal coliforms and phosphorus in water. *Construction and Building Materials, 93*, 1097–1104. https://doi.org/10.1016/j.conbuildmat.2015.05.034

Khaloo, A. R., Dehestani, M., & Rahmatabadi, P. (2008). Mechanical properties of concrete containing a high volume of tire-rubber particles. *Waste Management, 28*, 2472–2482. https://doi.org/10.1016/j.wasman.2008.01.015

Khed, V. C., Mohammed, B. S., Liew, M. S., & Abdullah Zawawi, N. A. W. (2020). Development of response surface models for self-compacting hybrid fibre reinforced rubberized cementitious composite. *Construction and Building Materials*. https://doi.org/10.1016/j.conbuildmat.2019.117191

Li, L. J., Tu, G. R., Lan, C., & Liu, F. (2016). Mechanical characterization of waste-rubber-modified recycled-aggregate concrete. *Journal of Cleaner Production, 124*, 325–338. https://doi.org/10.1016/j.jclepro.2016.03.003

Li, V. C., Shuxin, W., & Wu, C. (2001). Tensile strain-hardening behavior of polyvinyl alcohol engineered cementitious composite (PVA-ECC). *ACI Mater Journal, 98*, 483–492. https://doi.org/10.14359/10851

Li, V. C., Wu, C., Wang, S., Ogawa, A., & Saito, T. (2002). Interface tailoring for strain-hardening polyvinyl alcohol-engineered cementitious composite (PVA-ECC). *ACI Materials Journal, 99*, 463–472. https://doi.org/10.14359/12325

Liu, F., Zheng, W., Li, L., Feng, W., & Ning, G. (2013). Mechanical and fatigue performance of rubber concrete. *Construction and Building Materials, 47*, 711–719. https://doi.org/10.1016/j.conbuildmat.2013.05.055

Long, W. J., Li, H. D., Wei, J. J., Xing, F., & Han, N. (2018). Sustainable use of recycled crumb rubbers in eco-friendly alkali activated slag mortar: Dynamic mechanical properties. *Journal of Cleaner Production, 204*, 1004–1015. https://doi.org/10.1016/j.jclepro.2018.08.306

Magagula, S. I., Lebelo, K., Motloung, T. M., Mokhena, T. C., & Mochane, M. J. (2023). Recent advances on waste tires: Bibliometric analysis, processes, and waste management approaches. *Environmental Science and Pollution Research International, 30*, 118213–118245. https://doi.org/10.1007/s11356-023-30758-4

Magnusson, S., & Mácsik, J. (2017). Analysis of energy use and emissions of greenhouse gases, metals and organic substances from construction materials used for artificial turf. *Resources, Conservation and Recycling, 122*, 362–372. https://doi.org/10.1016/j.resconrec.2017.03.007

M.L. Mahlangu, (2009). Waste tyre management problems in South Africa and the possible opportunities that can be created through the recycling thereof, 124.

Meddah, M. S., & Bencheikh, M. (2009). Properties of concrete reinforced with different kinds of industrial waste fibre materials. *Construction and Building Materials, 23*, 3196–3205. https://doi.org/10.1016/j.conbuildmat.2009.06.017

Meyyappan, P. L., Anitha Selvasofia, S. D., Asmitha, M., Janani Praveena, S., & Simika, P. (2023). Experimental studies on partial replacement of crumb rubber as a fine aggregate in M30 grade concrete. *Materials Today: Proceedings, 74*, 985–992. https://doi.org/10.1016/j.matpr.2022.11.350

Mohammed, B. S., & Adamu, M. (2018). Mechanical performance of roller compacted concrete pavement containing crumb rubber and nano silica. *Construction and Building Materials, 159*, 234–251. https://doi.org/10.1016/j.conbuildmat.2017.10.098

Mohammed, B. S., Yen, L. Y., Haruna, S., Seng Huat, M. L., Abdulkadir, I., Al-Fakih, A., Liew, M. S., & Abdullah Zawawi, N. A. W. (2020). Effect of elevated temperature on the compressive strength and durability properties of crumb rubber engineered cementitious composite. *Materials*. https://doi.org/10.3390/MA13163516

Najim, K. B., & Hall, M. R. (2010). A review of the fresh/hardened properties and applications for plain- (PRC) and self-compacting rubberised concrete (SCRC). *Construction and Building Materials, 24*, 2043–2051. https://doi.org/10.1016/j.conbuildmat.2010.04.056

Noushini, A., Samali, B., & Vessalas, K. (2013). Effect of polyvinyl alcohol (PVA) fibre on dynamic and material properties of fibre reinforced concrete. *Construction and Building Materials, 49*, 374–383. https://doi.org/10.1016/j.conbuildmat.2013.08.035

Onuaguluchi, O., & Panesar, D. K. (2014). Hardened properties of concrete mixtures containing pre-coated crumb rubber and silica fume. *Journal of Cleaner Production, 82*, 125–131. https://doi.org/10.1016/j.jclepro.2014.06.068

Pham, N. P., Toumi, A., & Turatsinze, A. (2018). Rubber aggregate-cement matrix bond enhancement: Microstructural analysis, effect on transfer properties and on mechanical behaviours of the composite. *Cement and Concrete Composites, 94*, 1–12. https://doi.org/10.1016/j.cemconcomp.2018.08.005

Qaidi, S. M. A., Dinkha, Y. Z., Haido, J. H., Ali, M. H., & Tayeh, B. A. (2021). Engineering properties of sustainable green concrete incorporating eco-friendly aggregate of crumb rubber: A review. *Journal of Cleaner Production*. https://doi.org/10.1016/j.jclepro.2021.129251

Ren, F., Mo, J., Wang, Q., & Ho, J. C. M. (2022). Crumb rubber as partial replacement for fine aggregate in concrete: An overview. *Construction and Building Materials*. https://doi.org/10.1016/j.conbuildmat.2022.128049

Sgobba, S., Borsa, M., Molfetta, M., & Marano, G. C. (2015). Mechanical performance and medium-term degradation of rubberised concrete. *Construction and Building Materials, 98*, 820–831. https://doi.org/10.1016/j.conbuildmat.2015.07.095

Shahjalal, M., Islam, K., Rahman, J., Ahmed, K. S., Karim, M. R., & Billah, A. M. (2021). Flexural response of fiber reinforced concrete beams with waste tires rubber and recycled aggregate. *Journal of Cleaner Production*. https://doi.org/10.1016/j.jclepro.2020.123842

Shao, J., Zhu, H., Xue, G., Yu, Y., Mirgan Borito, S., & Jiang, W. (2021). Mechanical and restrained shrinkage behaviors of cement mortar incorporating waste tire rubber particles and expansive agent. *Construction and Building Materials*. https://doi.org/10.1016/j.conbuildmat.2021.123742

Shu, X., & Huang, B. (2014). Recycling of waste tire rubber in asphalt and Portland cement concrete: An overview. *Construction and Building Materials, 67*, 217–224. https://doi.org/10.1016/j.conbuildmat.2013.11.027

Siddika, A., Al Mamun, M. A., Alyousef, R., Amran, Y. H. M., Aslani, F., & Alabduljabbar, H. (2019). Properties and utilizations of waste tire rubber in concrete: A review. *Construction and Building Materials, 224*, 711–731. https://doi.org/10.1016/j.conbuildmat.2019.07.108

Singaravel, D. A., Veerapandian, P., Rajendran, S., & Dhairiyasamy, R. (2024). Enhancing high-performance concrete sustainability: integration of waste tire rubber for innovation. *Scientific Reports*. https://doi.org/10.1038/s41598-024-55485-9

Son, K. S., Hajirasouliha, I., & Pilakoutas, K. (2011). Strength and deformability of waste tyre rubber-filled reinforced concrete columns. *Construction and Building Materials, 25*, 218–226. https://doi.org/10.1016/j.conbuildmat.2010.06.035

H. Su, (2015) Properties of concrete with recycled aggregates as coarse aggregate and as-received/surface-modified rubber particles as fine aggregate in Civil Engineering. https://etheses.bham.ac.uk/id/eprint/6003/.

Tamanna, K., Tiznobaik, M., Banthia, N., & Shahria Alam, M. (2020). Mechanical properties of rubberized concrete containing recycled concrete aggregate. *ACI Materials Journal, 117*, 169–180. https://doi.org/10.14359/51722409

Thomas, B. S., Gupta, R. C., & Panicker, V. J. (2016). Recycling of waste tire rubber as aggregate in concrete: Durability-related performance. *Journal of Cleaner Production, 112*, 504–513. https://doi.org/10.1016/j.jclepro.2015.08.046

Toutanji, H. A. (1996). The use of rubber tire particles in concrete to replace mineral aggregates. *Cement and Concrete Composites, 18*, 135–139. https://doi.org/10.1016/0958-9465(95)00010-0

Turner, L. K., & Collins, F. G. (2013). Carbon dioxide equivalent (CO2-e) emissions: A comparison between geopolymer and OPC cement concrete. *Construction and Building Materials, 43*, 125–130. https://doi.org/10.1016/j.conbuildmat.2013.01.023

Udeze, O. J., Mohammed, B. S., Adebanjo, A. U., & Abdulkadir, I. (2024). Optimizing an eco-friendly high-density concrete for offshore applications: A study on fly ash partial replacement and graphene oxide nano reinforcement. *Case Studies in Chemical and Environmental Engineering*. https://doi.org/10.1016/j.cscee.2023.100592

Wang, J., Dai, Q., Si, R., & Guo, S. (2018). Investigation of properties and performances of polyvinyl alcohol (PVA) fiber-reinforced rubber concrete. *Construction and Building Materials, 193*, 631–642. https://doi.org/10.1016/j.conbuildmat.2018.11.002

Xie, J.-H., Xie, Z.-H., Liu, L.-S., & Guo, Y.-C. (2015). Compressive and flexural behaviours of a new steel-fibre-reinforced recycled aggregate concrete with crumb rubber. *Construction and Building Materials, 79*, 263–272. https://doi.org/10.1016/j.conbuildmat.2015.01.036

Xiong, C., Li, Q., Lan, T., Li, H., Long, W., & Xing, F. (2021). Sustainable use of recycled carbon fiber reinforced polymer and crumb rubber in concrete: mechanical properties and ecological evaluation. *Journal of Cleaner Production*. https://doi.org/10.1016/j.jclepro.2020.123624

Yang, K.-H., Song, J.-K., & Song, K.-I. (2013). Assessment of CO2 reduction of alkali-activated concrete. *Journal of Cleaner Production, 39*, 265–272.

Youssf, O., Hassanli, R., & Mills, J. E. (2017). Mechanical performance of FRP-confined and unconfined crumb rubber concrete containing high rubber content. *Journal of Building Engineering, 11*, 115–126. https://doi.org/10.1016/j.jobe.2017.04.011

Zhang, Y., & Aslani, F. (2021). Development of fibre reinforced engineered cementitious composite using polyvinyl alcohol fibre and activated carbon powder for 3D concrete printing. *Construction and Building Materials*. https://doi.org/10.1016/j.conbuildmat.2021.124453

Zheng, L., Sharon Huo, X., & Yuan, Y. (2008). Strength, modulus of elasticity, and brittleness index of rubberized concrete. *Journal of Materials in Civil Engineering., 20*, 692–699. https://doi.org/10.1061/(ASCE)0899-1561(2008)20:11(692)

Zhong, H., Poon, E. W., Chen, K., & Zhang, M. (2019). Engineering properties of crumb rubber alkali-activated mortar reinforced with recycled steel fibres. *Journal of Cleaner Production*. https://doi.org/10.1016/j.jclepro.2019.117950

Zhu, H., Chen, W., Cheng, S., Yang, L., Wang, S., & Xiong, J. (2022). Low carbon and high efficiency limestone-calcined clay as supplementary cementitious materials (SCMs): Multi-indicator comparison with conventional SCMs. *Construction and Building Materials*. https://doi.org/10.1016/j.conbuildmat.2022.127748

Zhu, H., Wang, Z., Xu, J., & Han, Q. (2019). Microporous structures and compressive strength of high-performance rubber concrete with internal curing agent. *Construction and Building Materials, 215*, 128–134. https://doi.org/10.1016/j.conbuildmat.2019.04.184

Zia, A., & Ali, M. (2017). Behavior of fiber reinforced concrete for controlling the rate of cracking in canal-lining. *Construction and Building Materials, 155*, 726–739. https://doi.org/10.1016/j.conbuildmat.2017.08.078

Publisher's Note

Naraindas Bheel (PhD student, Civil and Environmental Engineering Department, Universiti Teknologi PETRONAS, Malaysia)

Abhijeet Vidyadhar Baikerikar (PhD student, Civil and Environmental Engineering Department, Universiti Teknologi PETRONAS, Malaysia)

Bashar S. Mohammed (Associate Professor (Main Supervisor), Civil and Environmental Engineering Department, Universiti Teknologi PETRONAS, Malaysia).